Supporting Information file

For

Regio- and Stereo-Specific Electrophilic Addition of $TeBr_4$ and $ArylTeBr_3$ across Terminal Acetylenes Bond

Puspendra Singh,[*,1] Swami Nath Bharti,[2] Andrew Duthie,[3] Ray J. Butcher[4]

[1]Department of Chemistry, Dr. Shakuntala Misra National Rehabilitation University, Lucknow, 226017, India.

[2]Department of Chemistry, University of Lucknow, Lucknow, 226007, India.

[3]School of Life and Environmental Sciences, Deakin University, Geelong, 3217, Australia.

[4]Department of Chemistry, Howard University, Washington DC 20059, USA.

*Corresponding Author, E-mail address: pushpendrasingh0612@gmail.com

INDEX

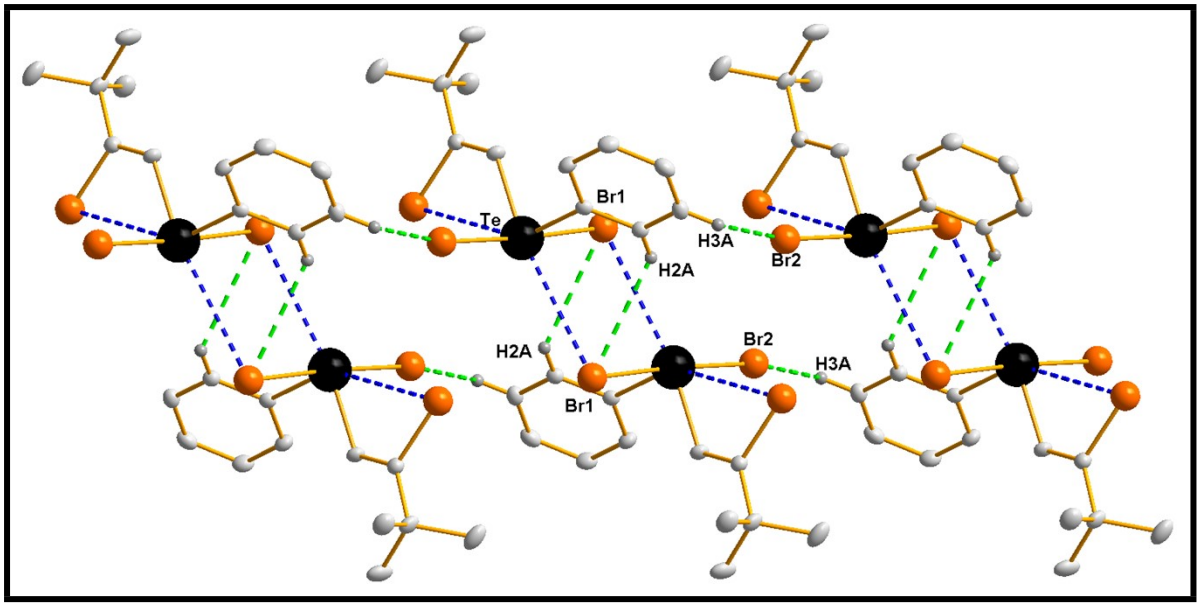

Fig. S1 Supramolecular aggregates sustained by Br(lp)···Te, [3.366(1) to 3.604(0) Å] NBIs and C-H···Br [C2-H2A···Br1, 3.095(0) Å and C3-H3A···Br2, 3.049(0) Å] HBIs in the crystal structures of **2**. Hydrogen atoms are omitted for clarity of the figure.

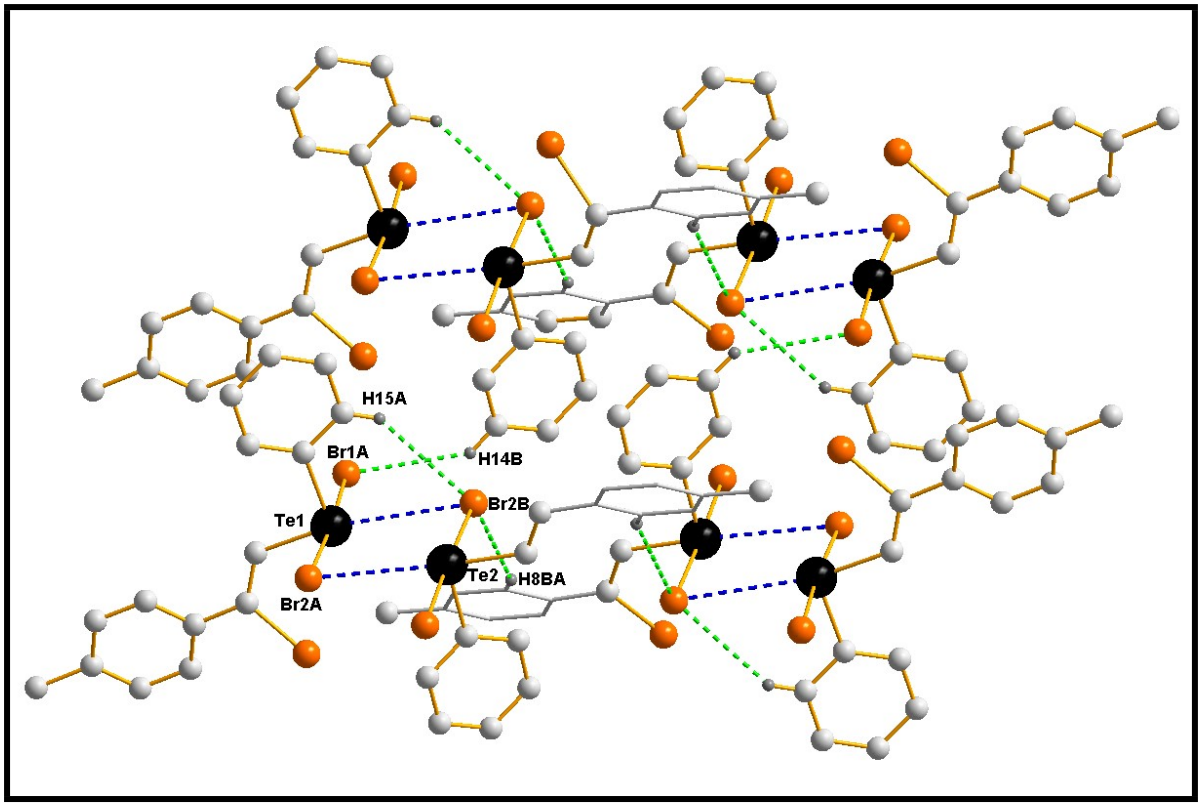

Fig. S2 Supramolecular aggregates sustained by Br(lp)···Te, [3.373(1) to 3.707(11) Å] NBIs and C-H···Br [C8B-HBA···Br2B, 3.184(1); C14B-H14B···Br1A, 3.049(1); C15A-H15A···Br2B, 3.087(1) Å] HBIs in the crystal structures of **7**. Hydrogen atoms are omitted for clarity of the figure.

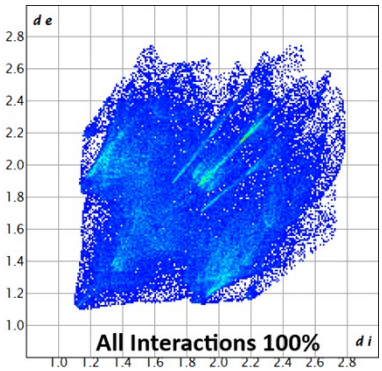
d e
All Interactions 100%
d i

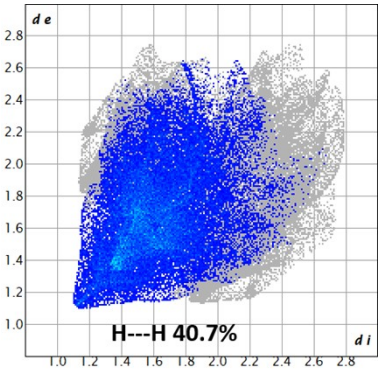
d e
H---H 40.7%
d i

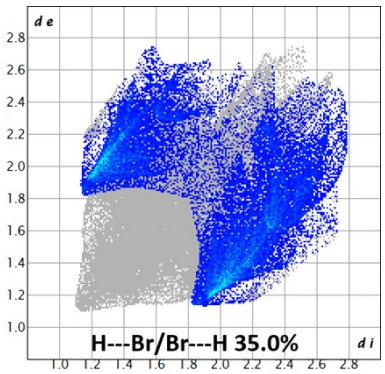
d e
H---Br/Br---H 35.0%
d i

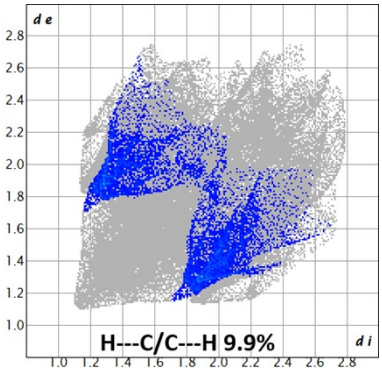
d e
H---C/C---H 9.9%
d i

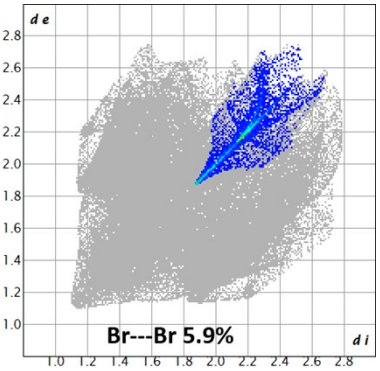
d e
Br---Br 5.9%
d i

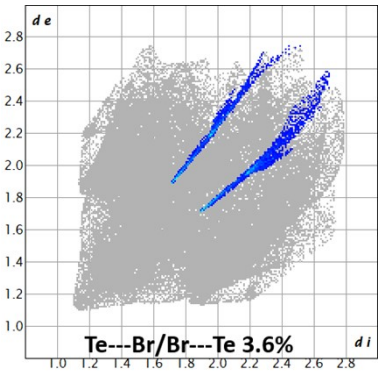
d e
Te---Br/Br---Te 3.6%
d i

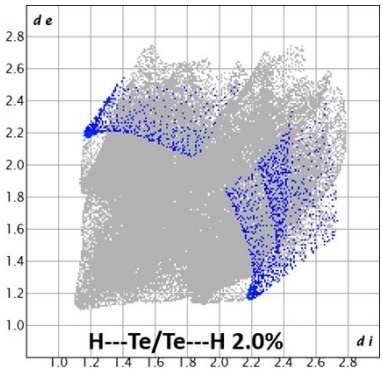
d e
H---Te/Te---H 2.0%
d i

Fig. S3 Full and decomposed 2D fingerprint plots of compound **2.**

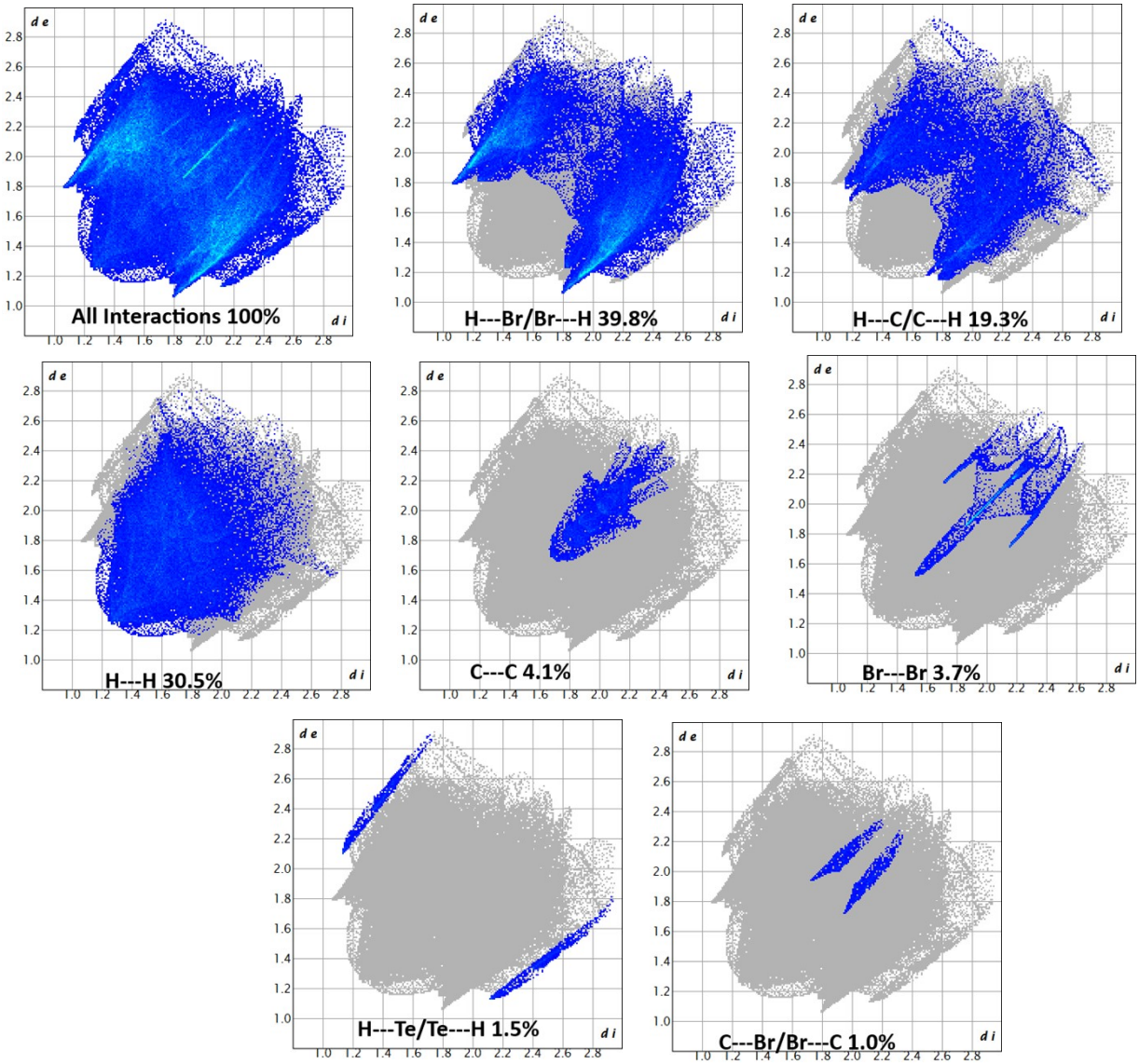
All Interactions 100%
H---Br/Br---H 39.8%
H---C/C---H 19.3%
H---H 30.5%
C---C 4.1%
Br---Br 3.7%
H---Te/Te---H 1.5%
C---Br/Br---C 1.0%
d e
d i

Fig. S4 Full and decomposed 2D fingerprint plots of compound **7.**

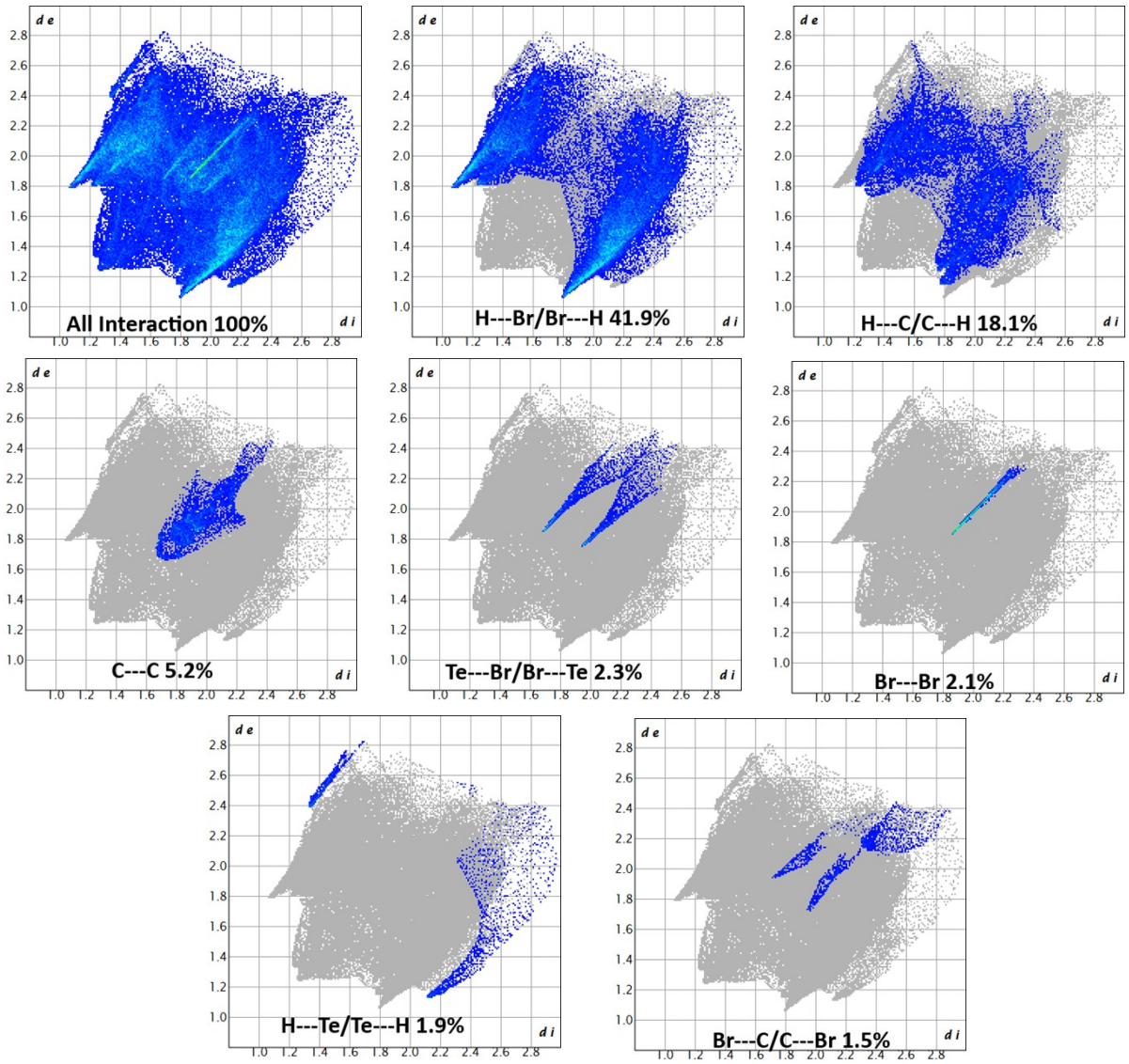
All Interaction 100%
H---Br/Br---H 41.9%
H---C/C---H 18.1%
C---C 5.2%
Te---Br/Br---Te 2.3%
Br---Br 2.1%
H---Te/Te---H 1.9%
Br---C/C---Br 1.5%
d e
d i

Fig. S5 Full and decomposed 2D fingerprint plots of molecule A of compound **7.**

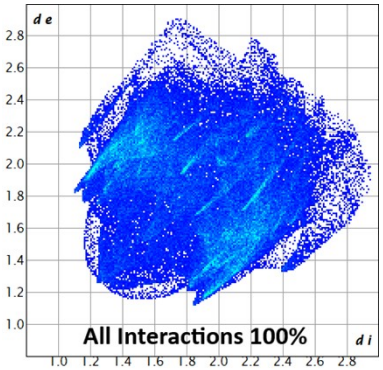
d e
d i
All Interactions 100%

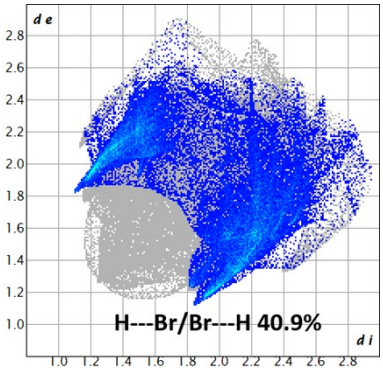
d e
d i
H---Br/Br---H 40.9%

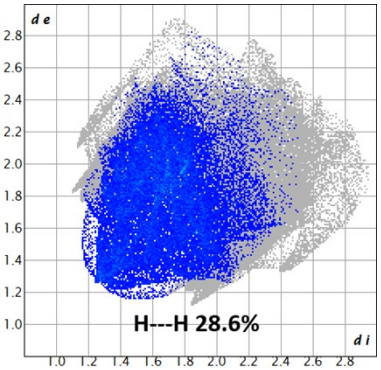
d e
d i
H---H 28.6%

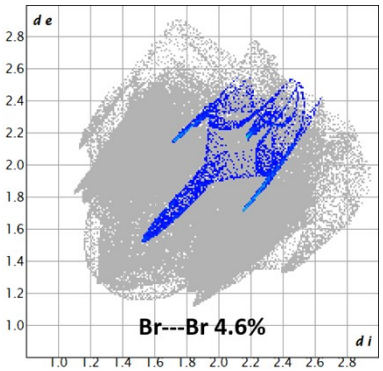
d e
d i
Br---Br 4.6%

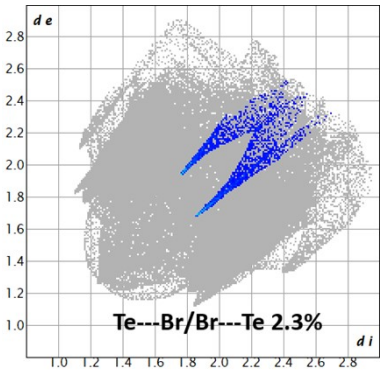
d e
d i
Te---Br/Br---Te 2.3%

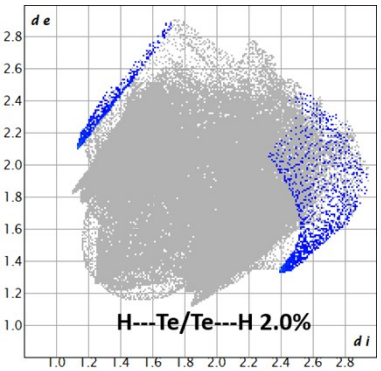
d e
d i
H---Te/Te---H 2.0%

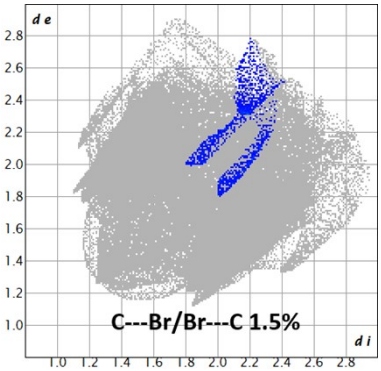
d e
d i
C---Br/Br---C 1.5%

Fig. S6 Full and decomposed 2D fingerprint plots of molecule B of compound **7.**

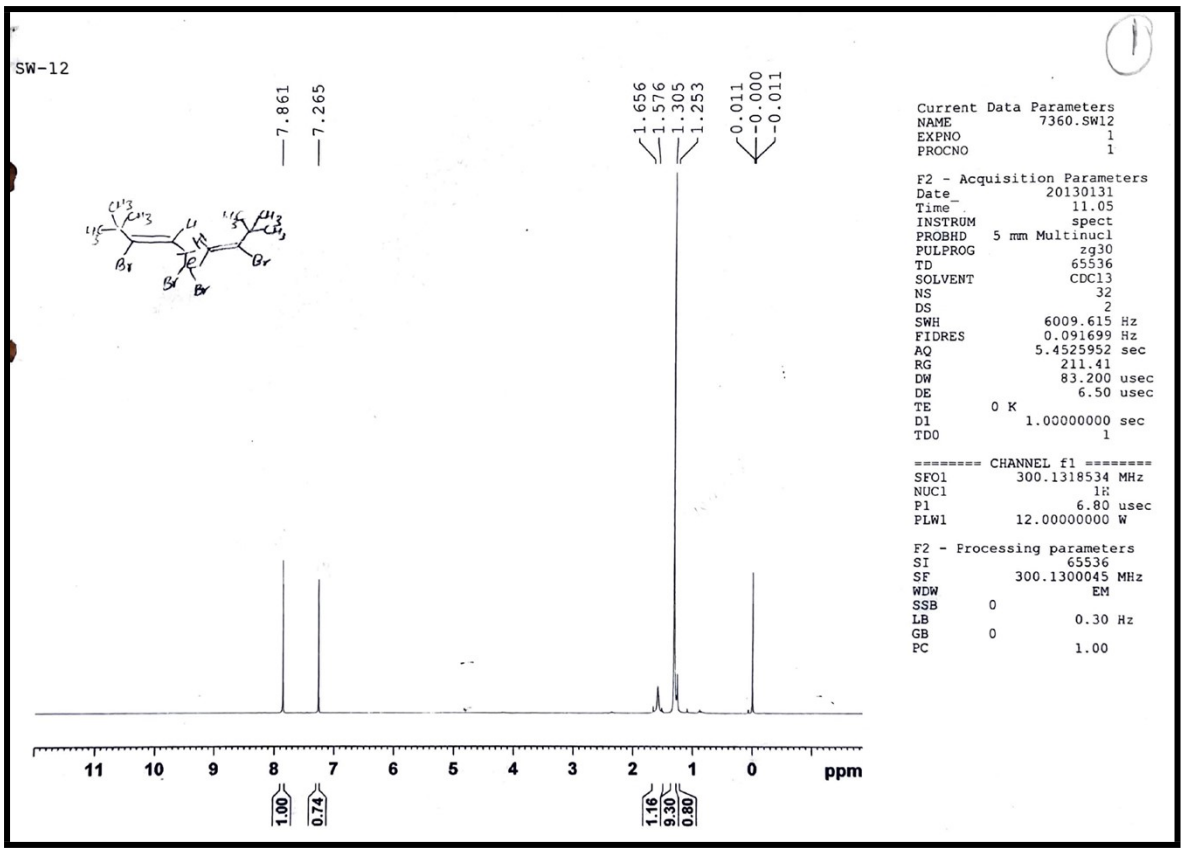

Fig. S7 ^{1}H NMR spectrum of [*t*-BuC(Br)=CH]$_2$TeBr$_2$ (**1**).

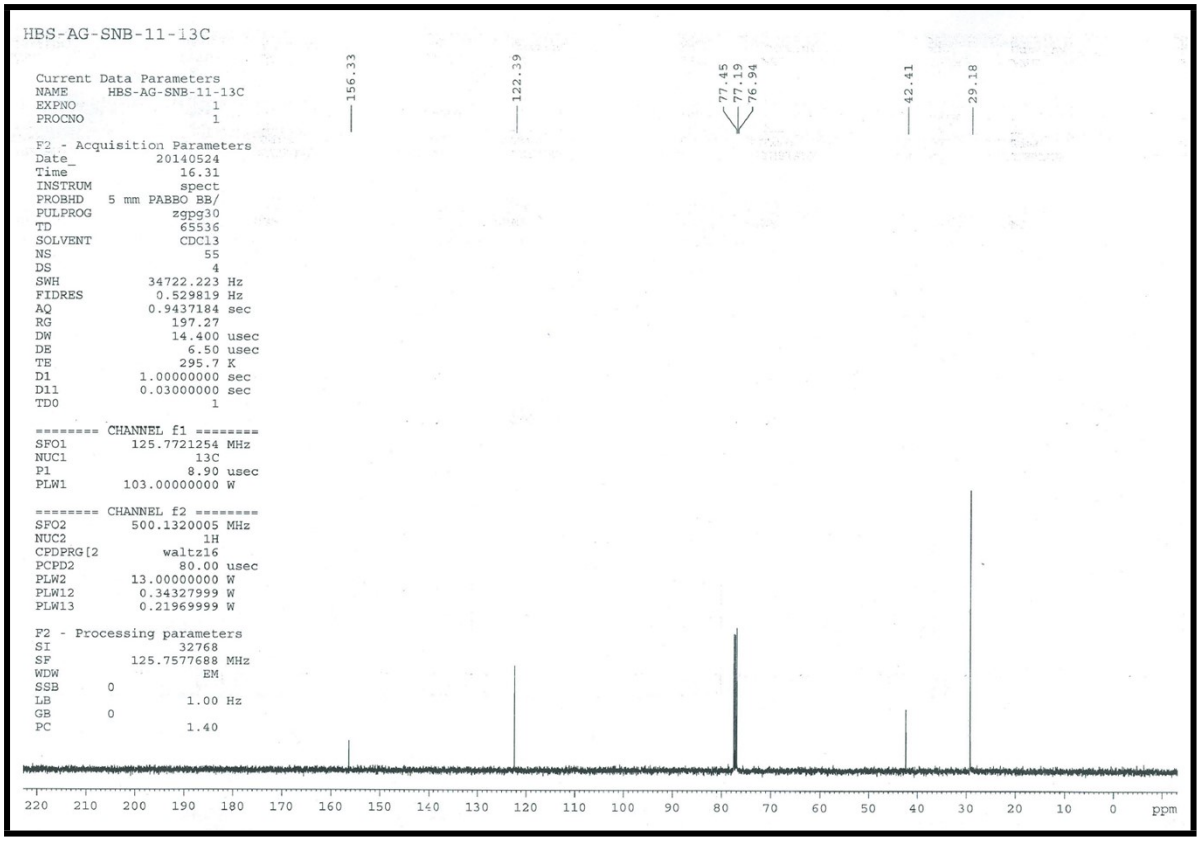

Fig. S8 ^{13}C NMR spectrum of [*t*-BuC(Br)=CH]$_2$TeBr$_2$ (**1**).

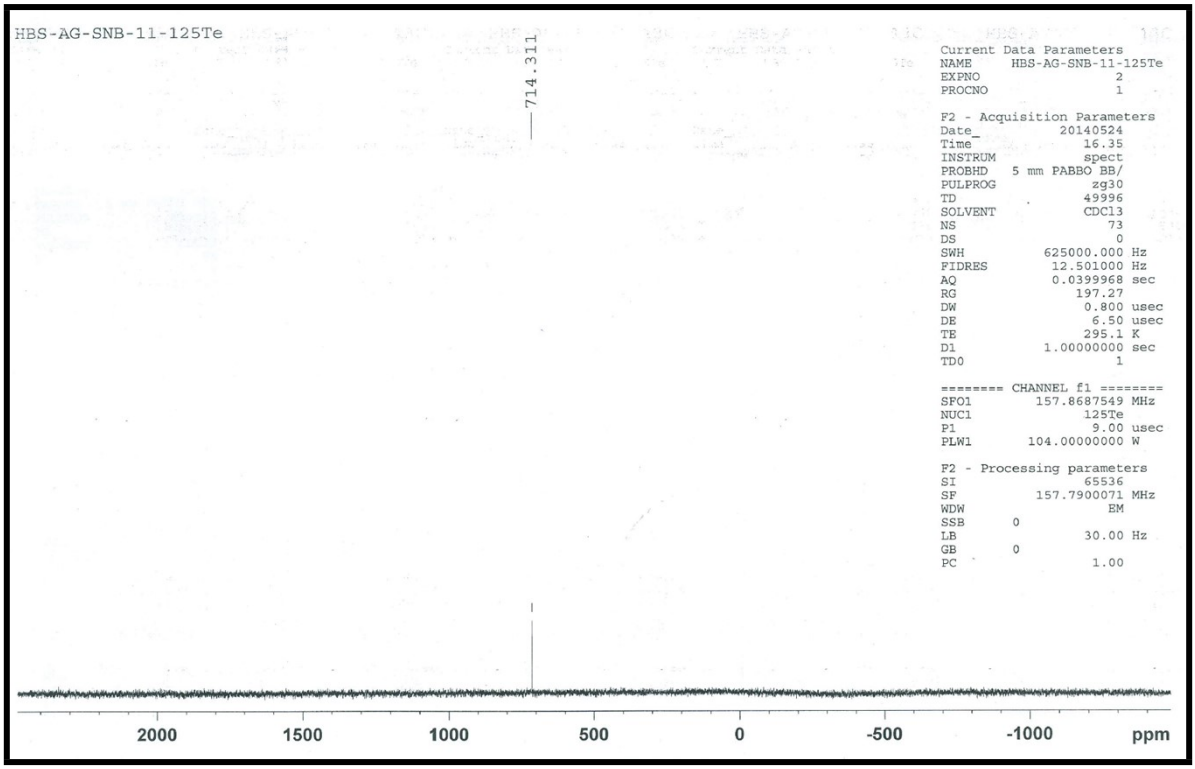

Fig. S9 ^{125}Te NMR spectrum of [*t*-BuC(Br)=CH]$_2$TeBr$_2$ (**1**).

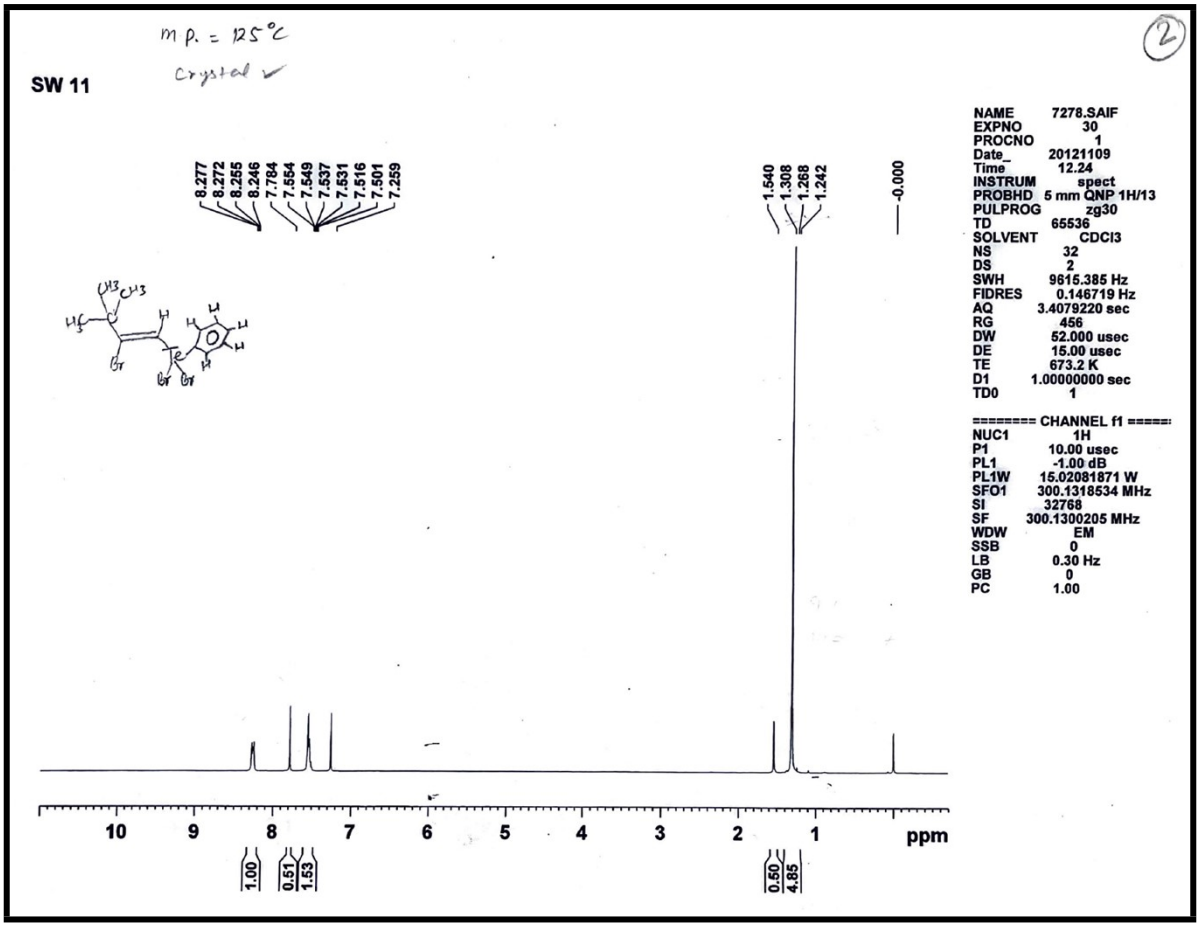

Fig. S10 ^{1}H NMR spectrum of [(C_6H_5)-{*t*-BuC(Br)=CH}]$TeBr_2$ (**2**).

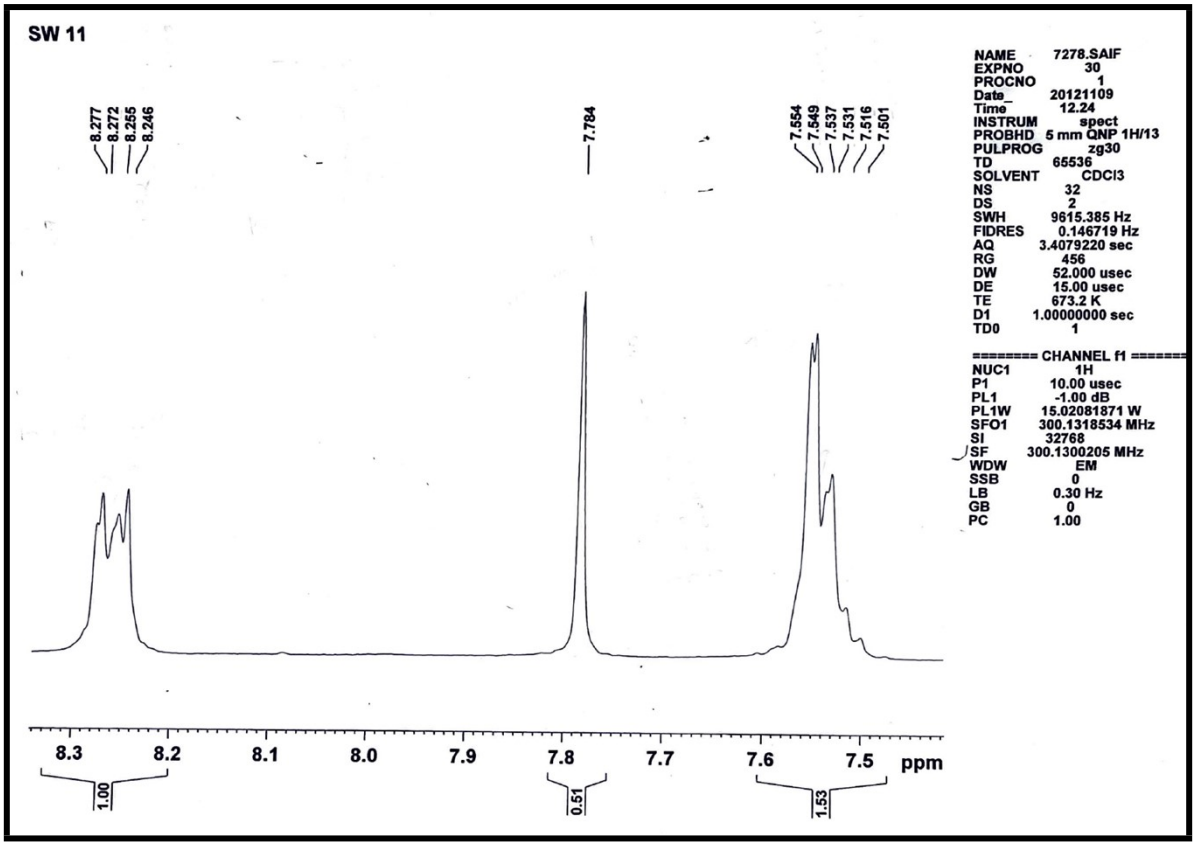

Fig. S11 Expanded aryl region of ^{1}H NMR spectrum of [(C_6H_5)-{*t*-BuC(Br)=CH}]$TeBr_2$ (**2**).

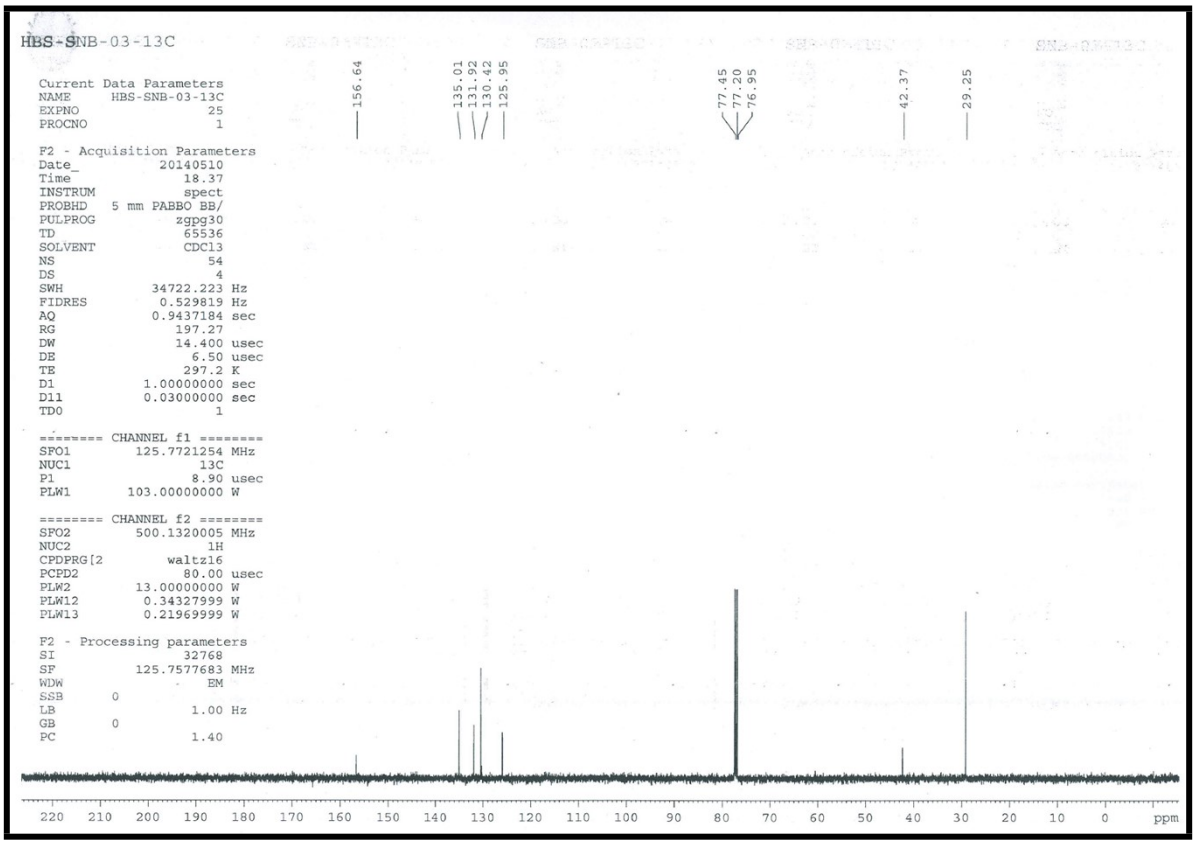

Fig. S12 ^{13}C NMR spectrum of $[(C_6H_5)\text{-}\{t\text{-BuC(Br)=CH}\}]TeBr_2$ (**2**).

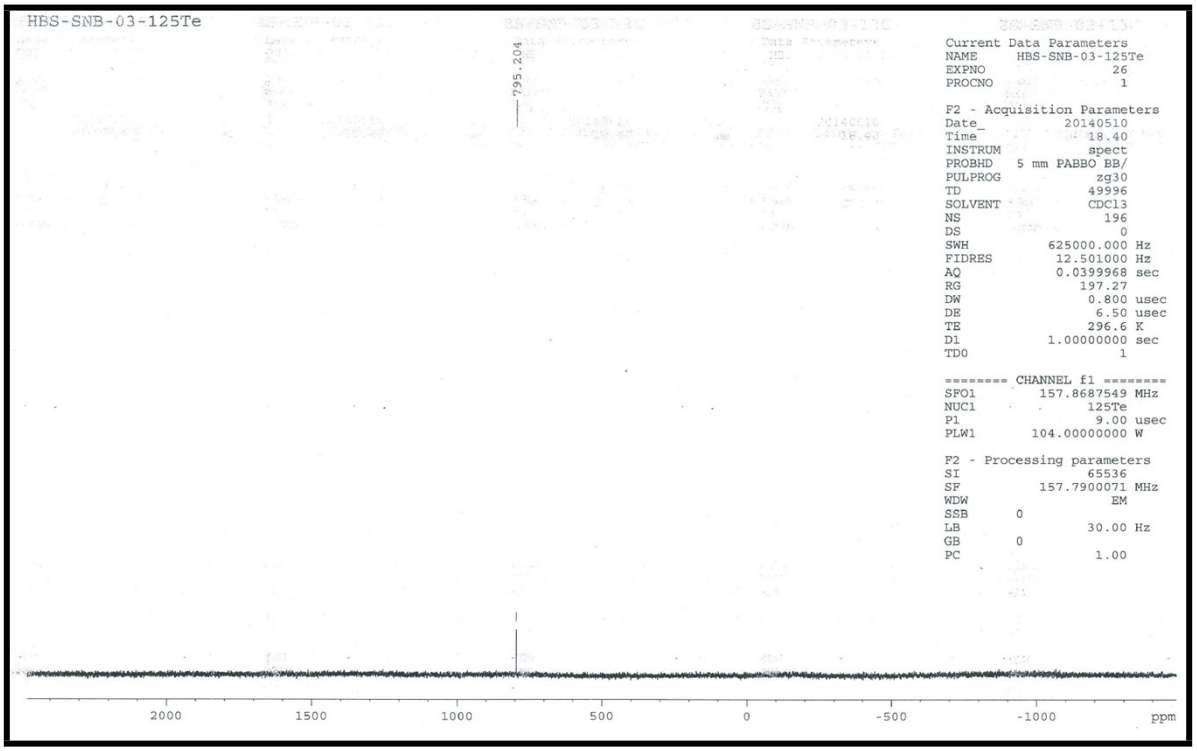

Fig. S13 ^{125}Te NMR spectrum of $[(C_6H_5)\text{-}\{t\text{-BuC(Br)=CH}\}]TeBr_2$ (**2**).

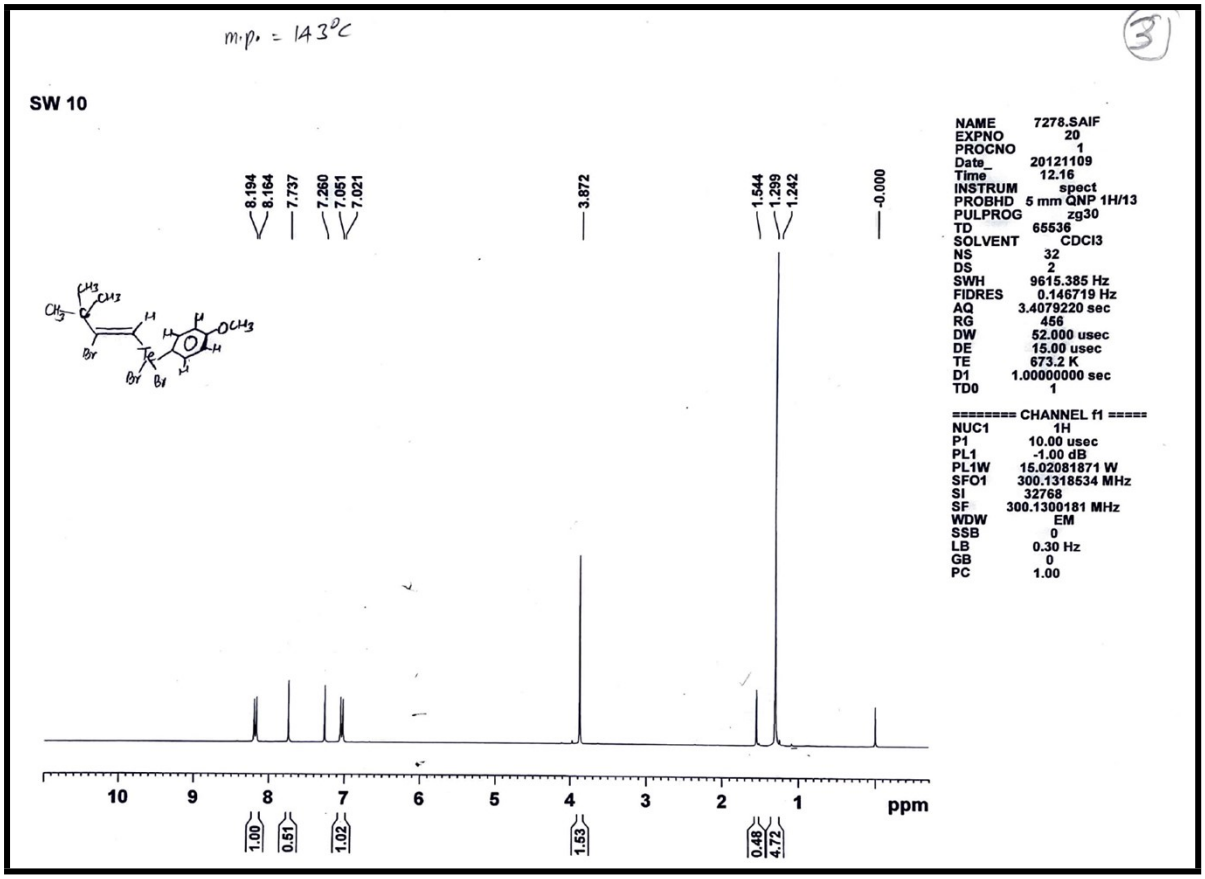

Fig. S14 ^{1}H NMR spectrum of [(*4*-MeOC$_6$H$_4$)-{*t*-Bu(C(Br)=CH}]TeBr$_2$ (**3**).

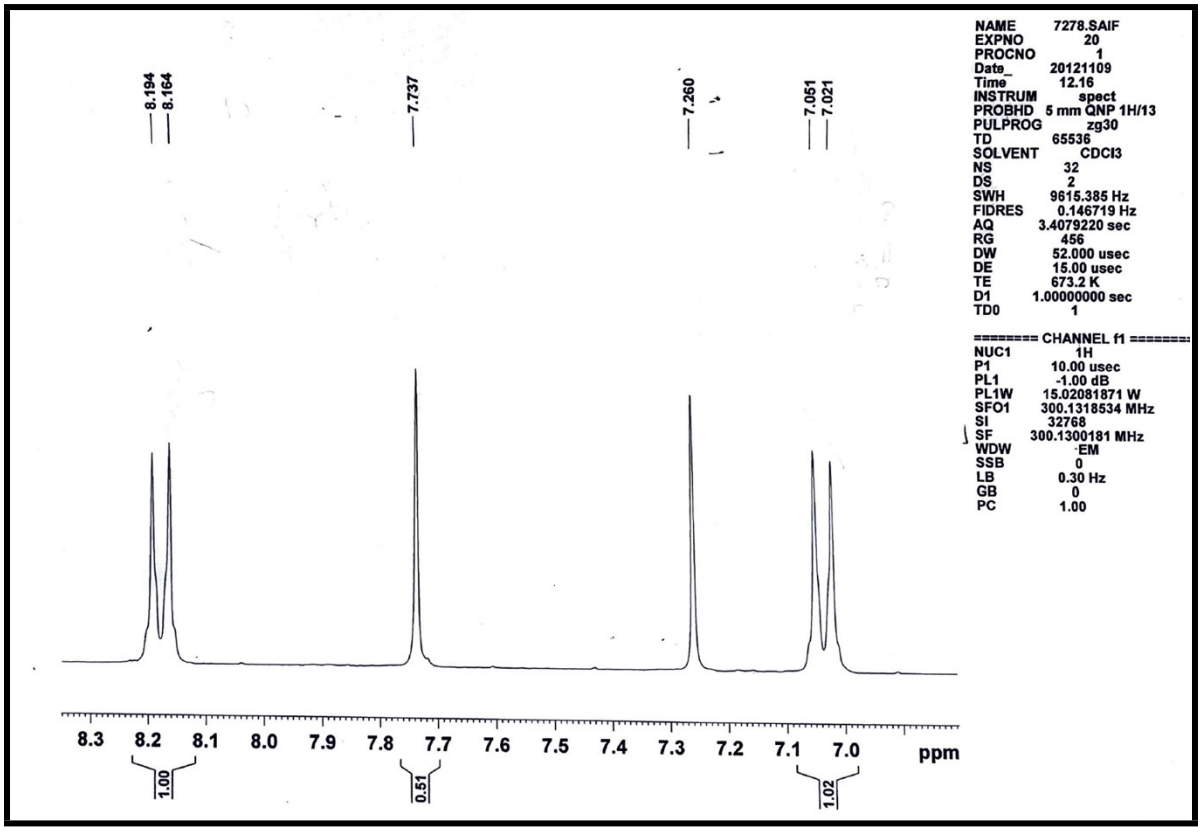

Fig. S15 Expanded aryl region of ^{1}H NMR spectrum of [(*4*-MeOC$_6$H$_4$)-{*t*-Bu(C(Br)=CH}]TeBr$_2$ (**3**).

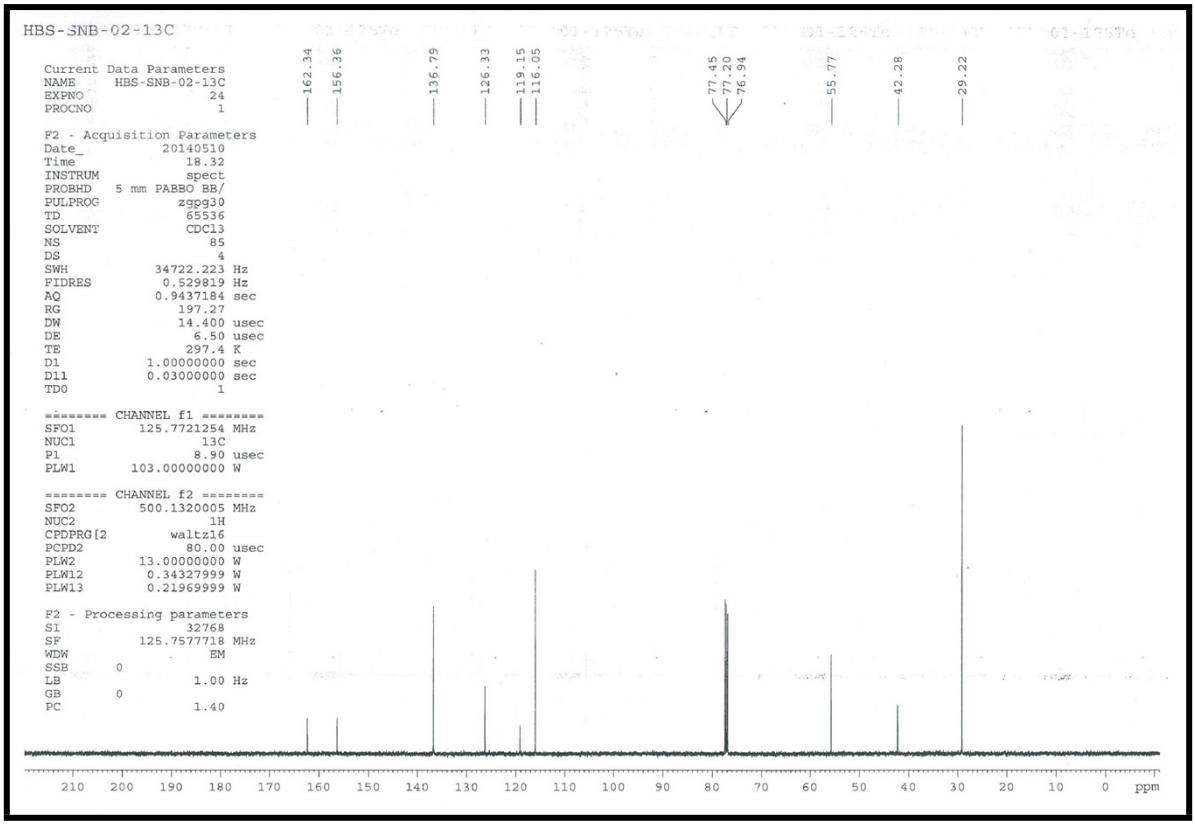

Fig. S16 ^{13}C NMR spectrum of [(*4*-MeOC$_6$H$_4$)-{*t*-Bu(C(Br)=CH}]TeBr$_2$ (**3**).

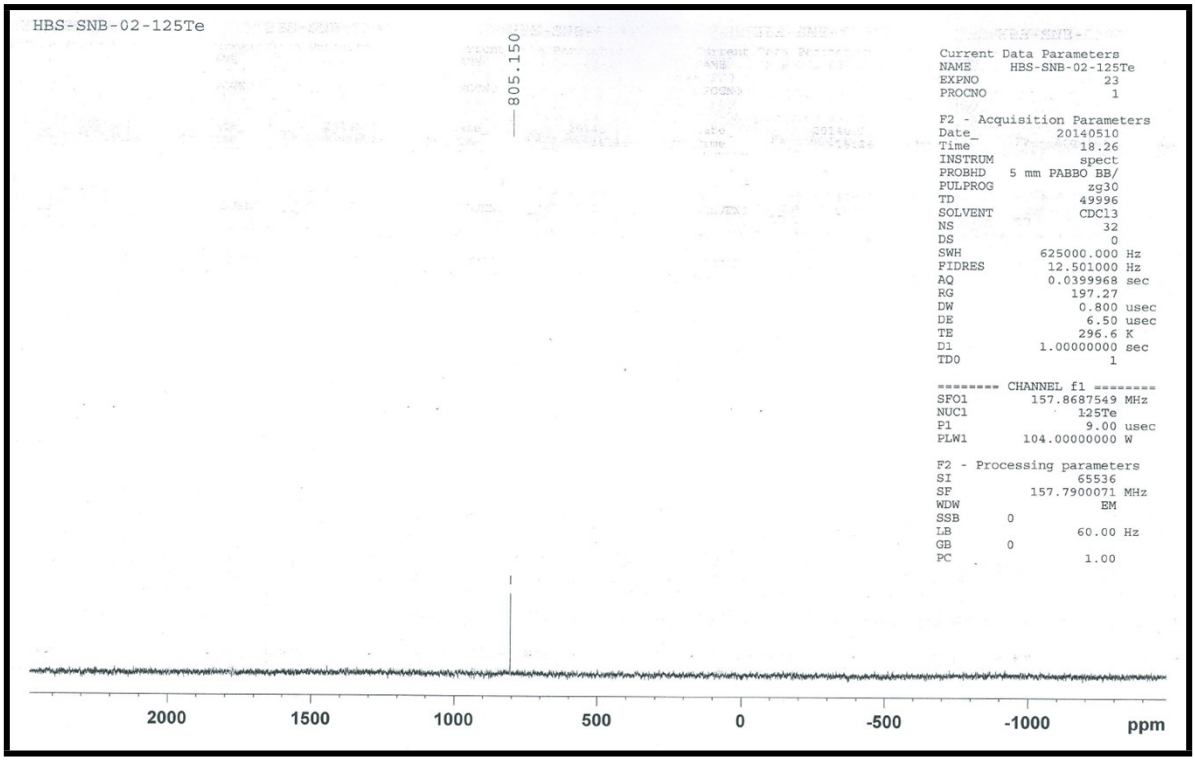

Fig. S17 ^{125}Te NMR spectrum of [(*4*-MeOC$_6$H$_4$)-{*t*-Bu(C(Br)=CH}]TeBr$_2$ (**3**).

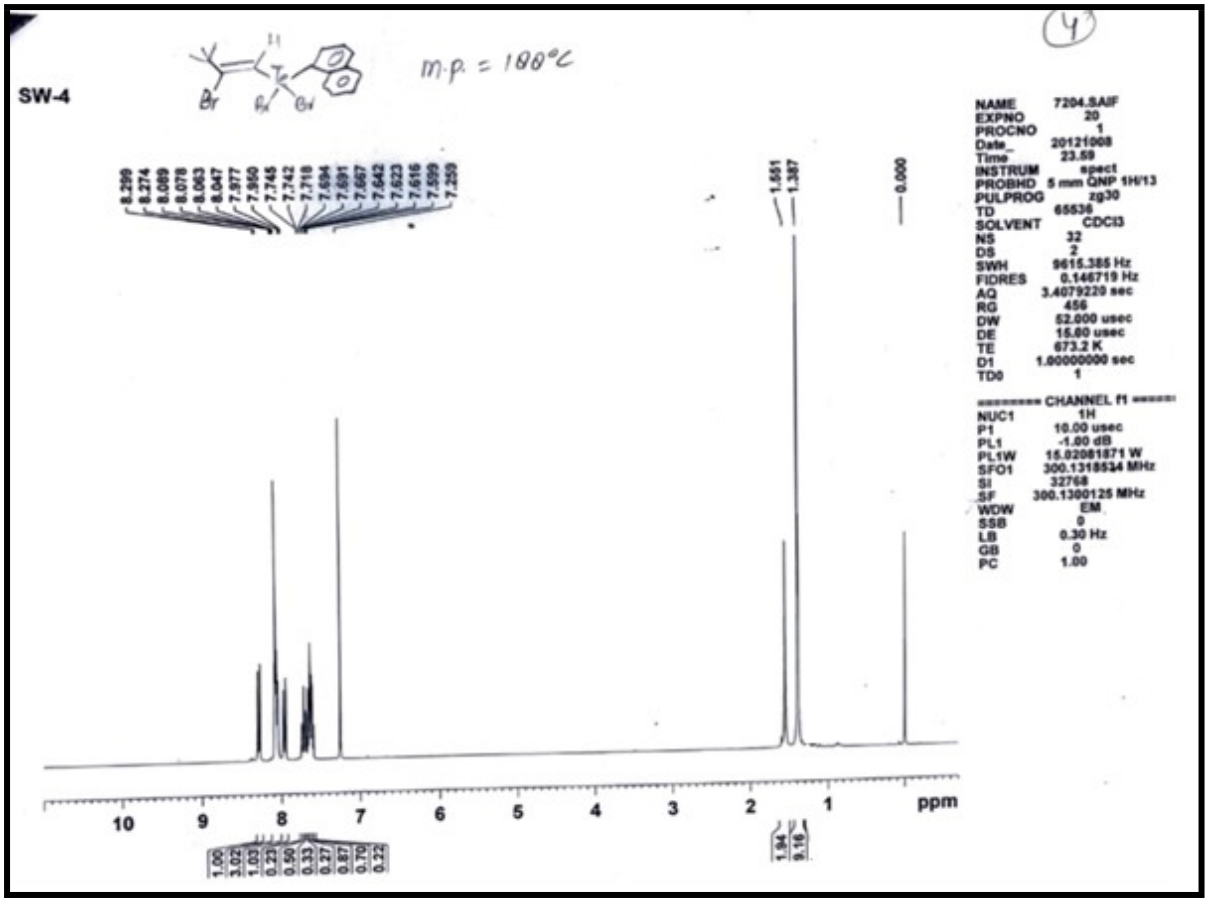

Fig. S18 ^{1}H NMR spectrum of [(*1*-$C_{10}H_7$)-{*t*-BuC(Br)=CH}]$TeBr_2$ (**4**).

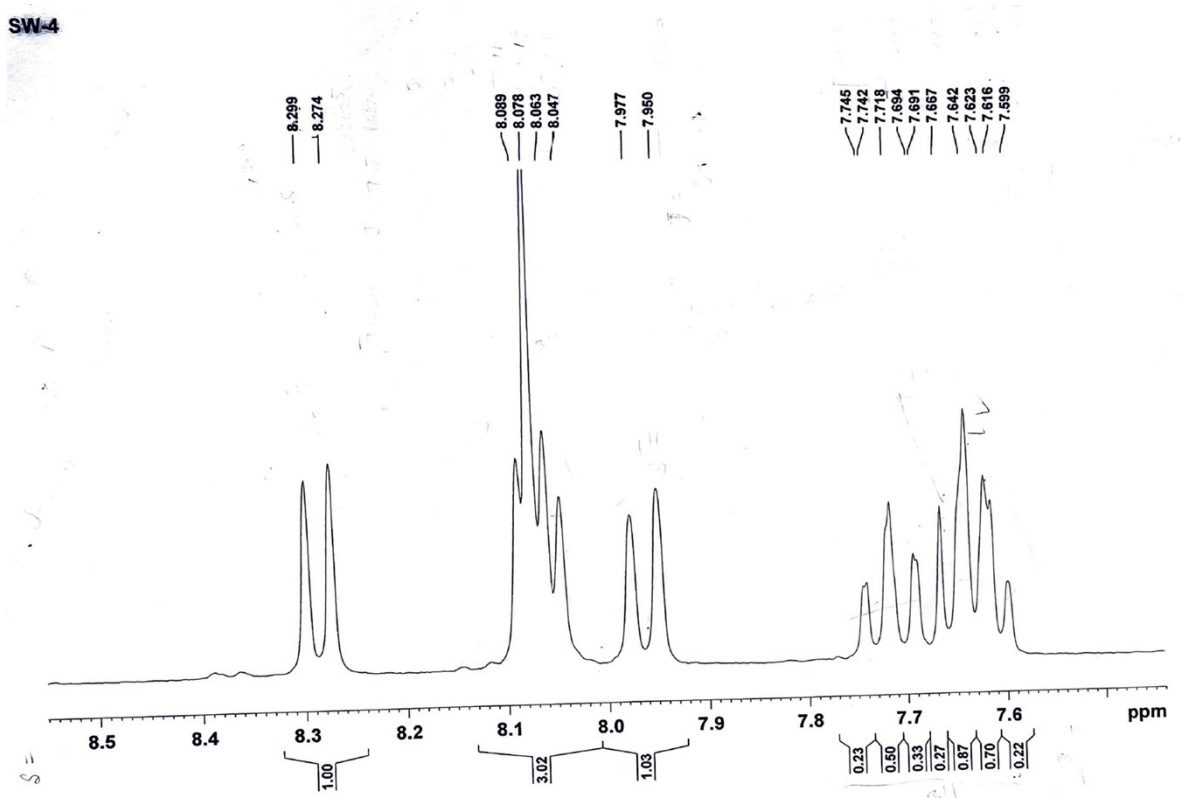

Fig. S19 Expanded aryl region of ^{1}H NMR spectrum of [(*1*-$C_{10}H_7$)-{*t*-Bu(C(Br)=CH}]$TeBr_2$ (**4**).

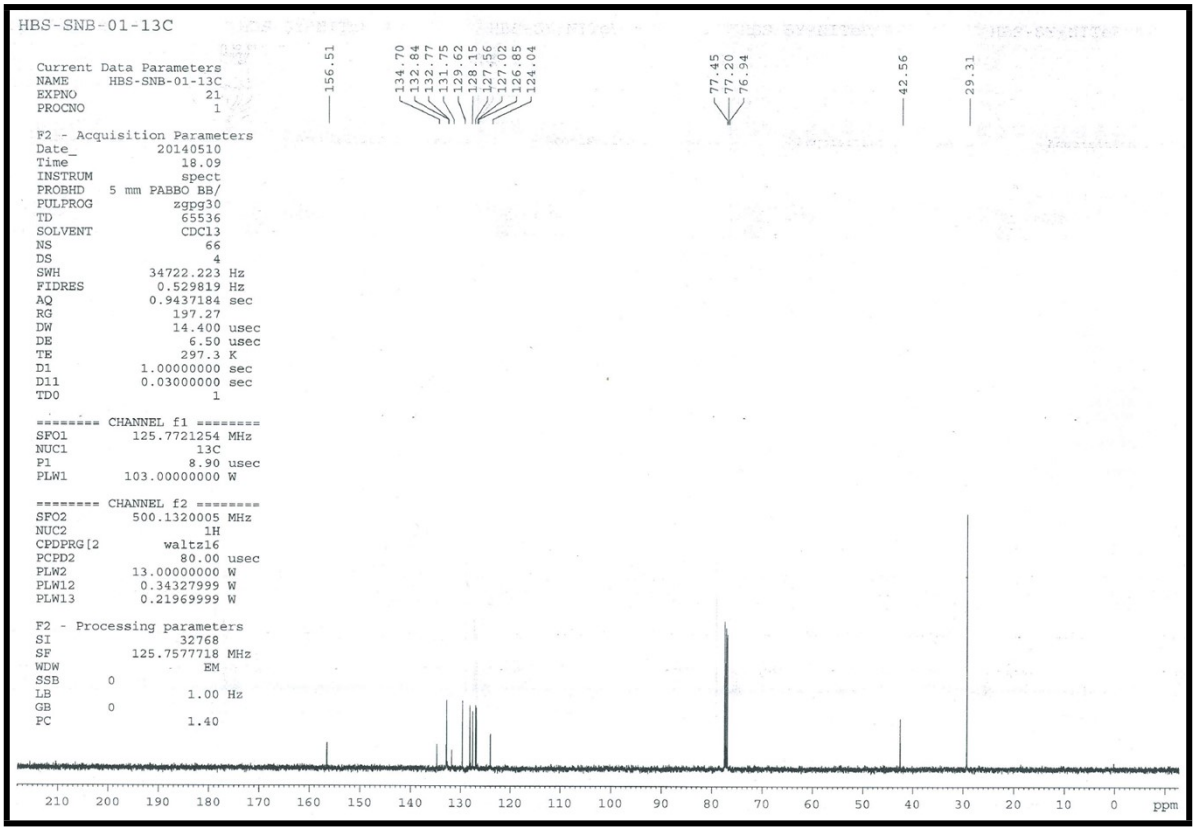

Fig. S20 ^{13}C NMR spectrum of [(*1*-$C_{10}H_7$)-{*t*-BuC(Br)=CH}]$TeBr_2$ (**4**).

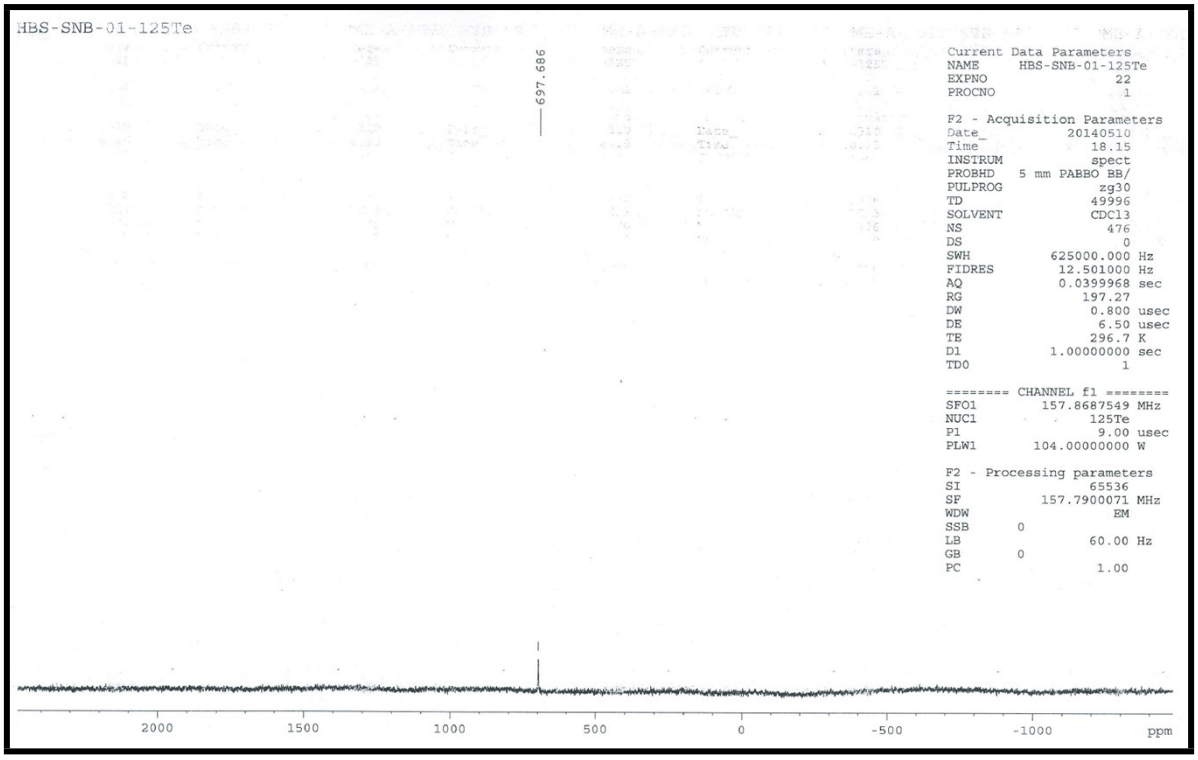

Fig. S21 ^{125}Te NMR spectrum of [(*1*-$C_{10}H_7$)-{*t*-Bu(C(Br)=CH}]$TeBr_2$ (**4**).

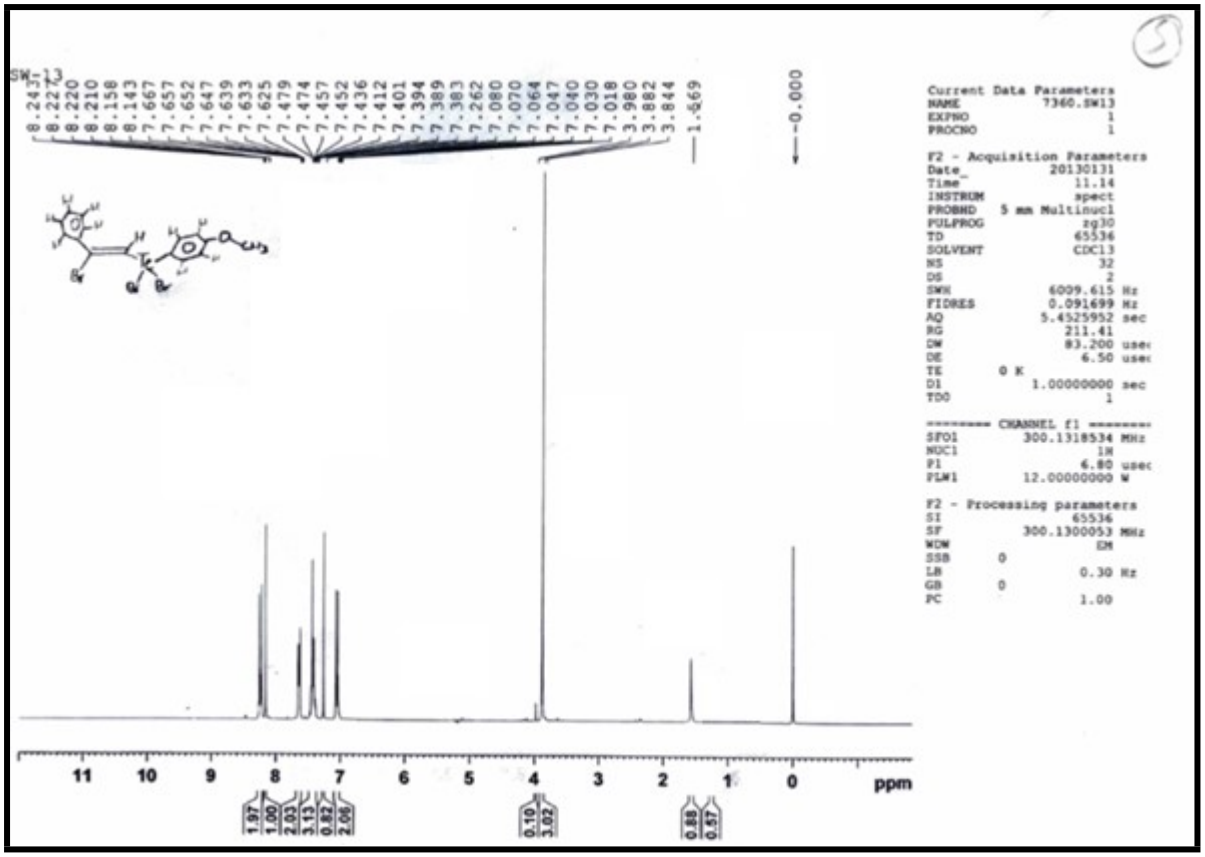

Fig. S22 ^{1}H NMR spectrum of [(*4*-$CH_3OC_6H_4$)-{$C_6H_5C(Br)=CH$}]$TeBr_2$ (**5**).

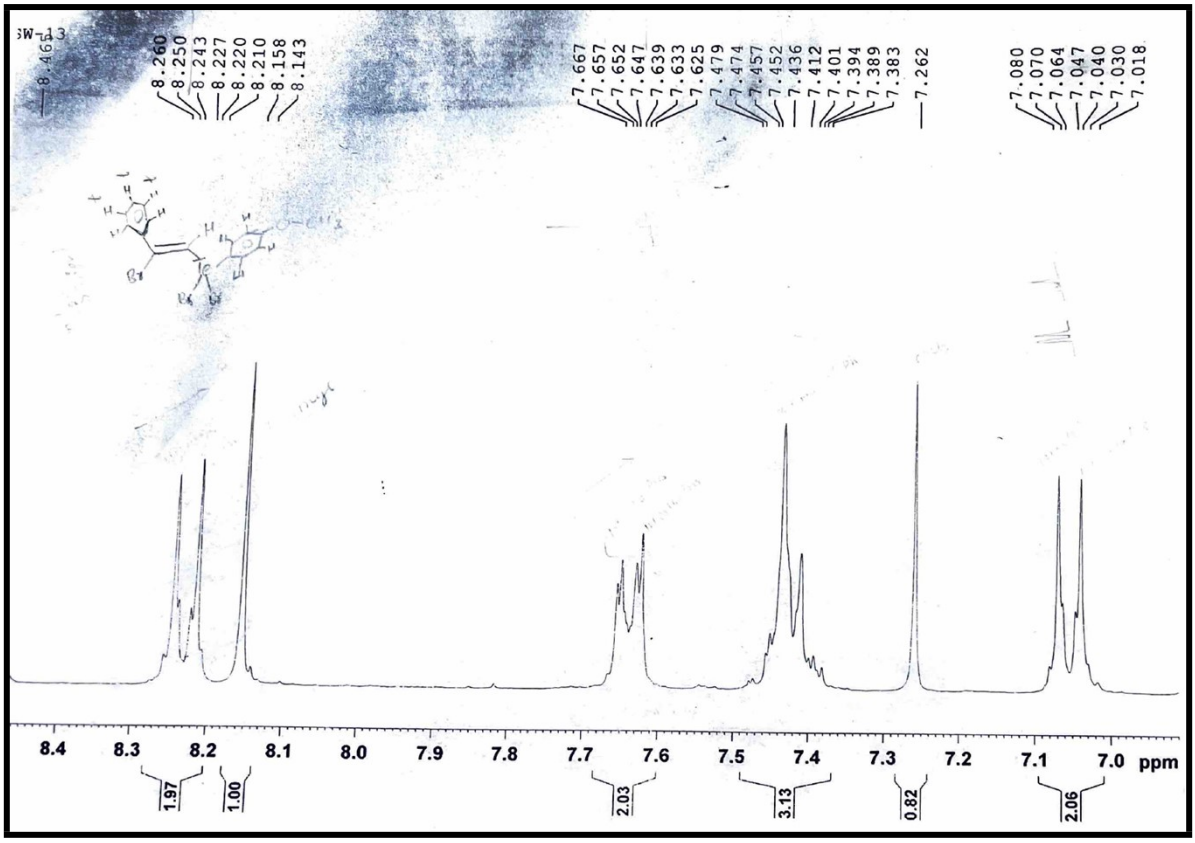

Fig. S23 Expanded aryl region of ^{1}H NMR spectrum of [(*4*-$CH_3OC_6H_4$)-{$C_6H_5C(Br)=CH$}]$TeBr_2$ (**5**).

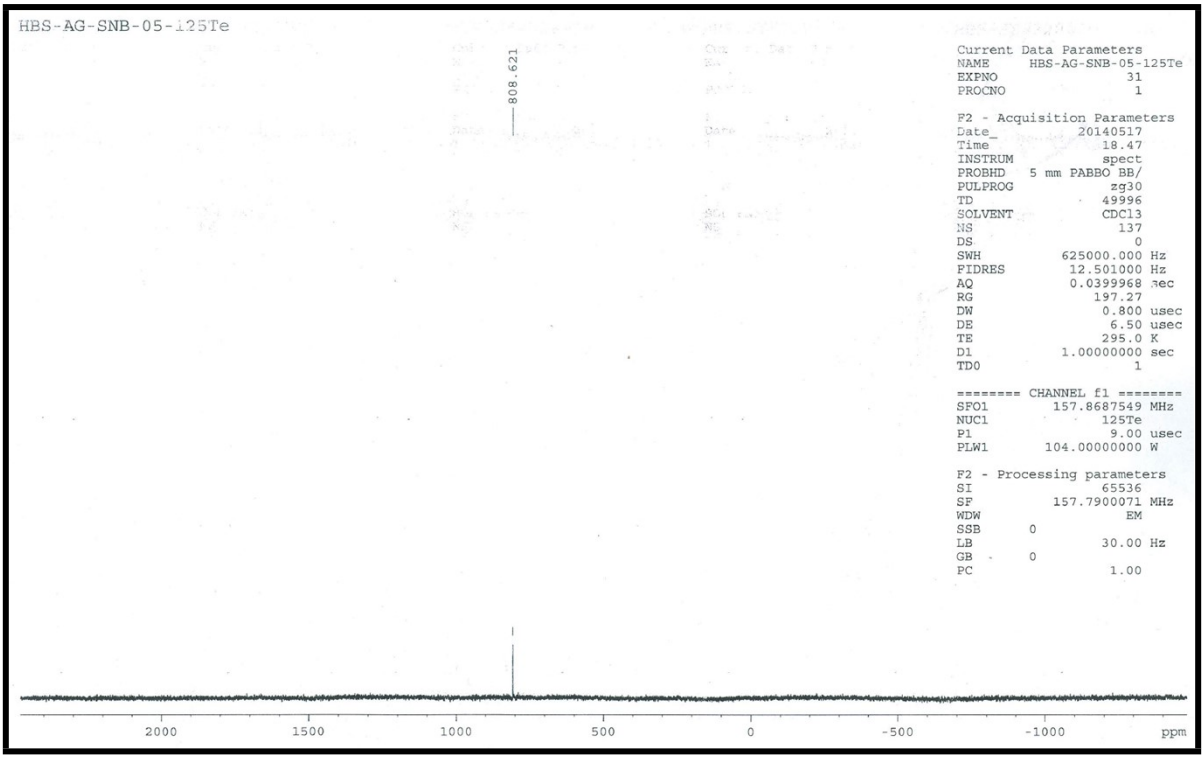

Fig. S24 ^{125}Te NMR spectrum of [(*4*-$CH_3OC_6H_4$)-{C_6H_5(C(Br)=CH}]$TeBr_2$ (**5**).

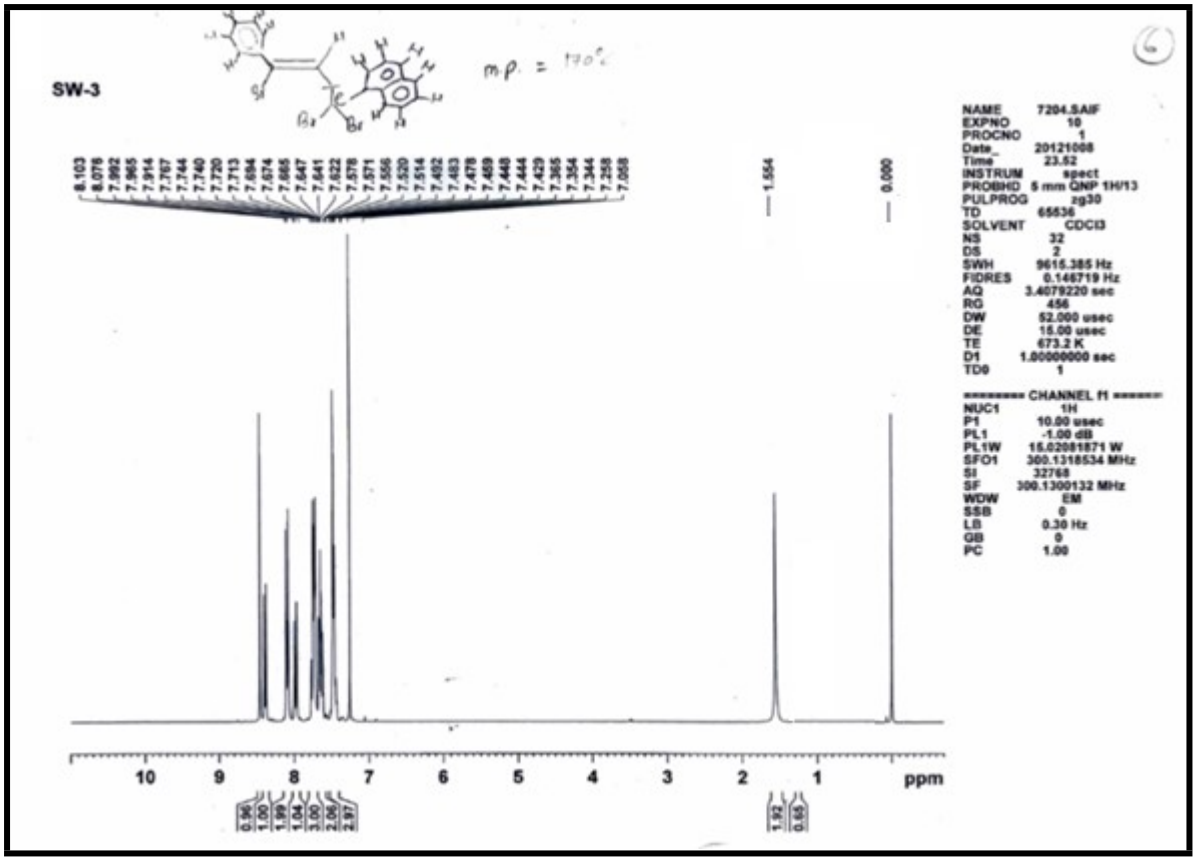

Fig. S25 ^{1}H NMR spectrum of [(*1*-$C_{10}H_7$)-{$C_6H_5C(Br)=CH$}]$TeBr_2$ (**6**).

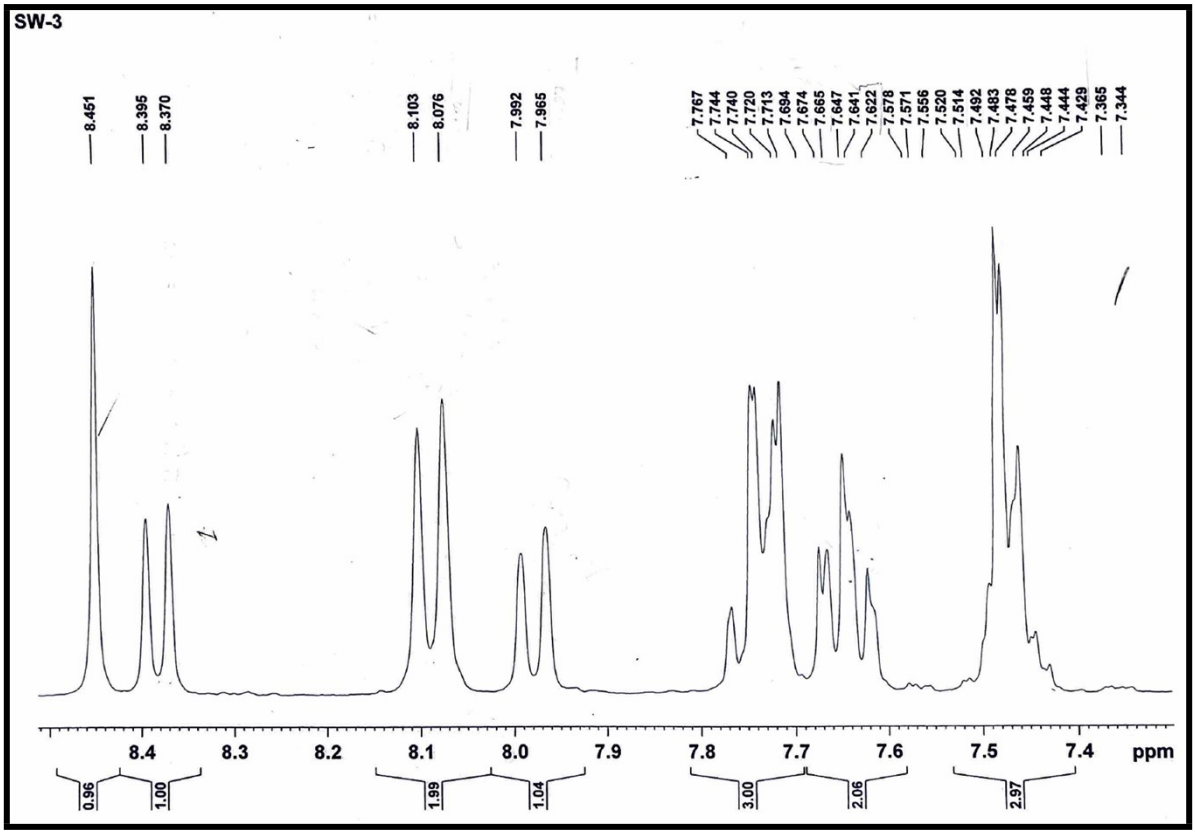

Fig. S26 Expanded aryl region of ^{1}H NMR spectrum of [(*1*-$C_{10}H_7$)-{$C_6H_5C(Br)=CH$}]$TeBr_2$ (**6**).

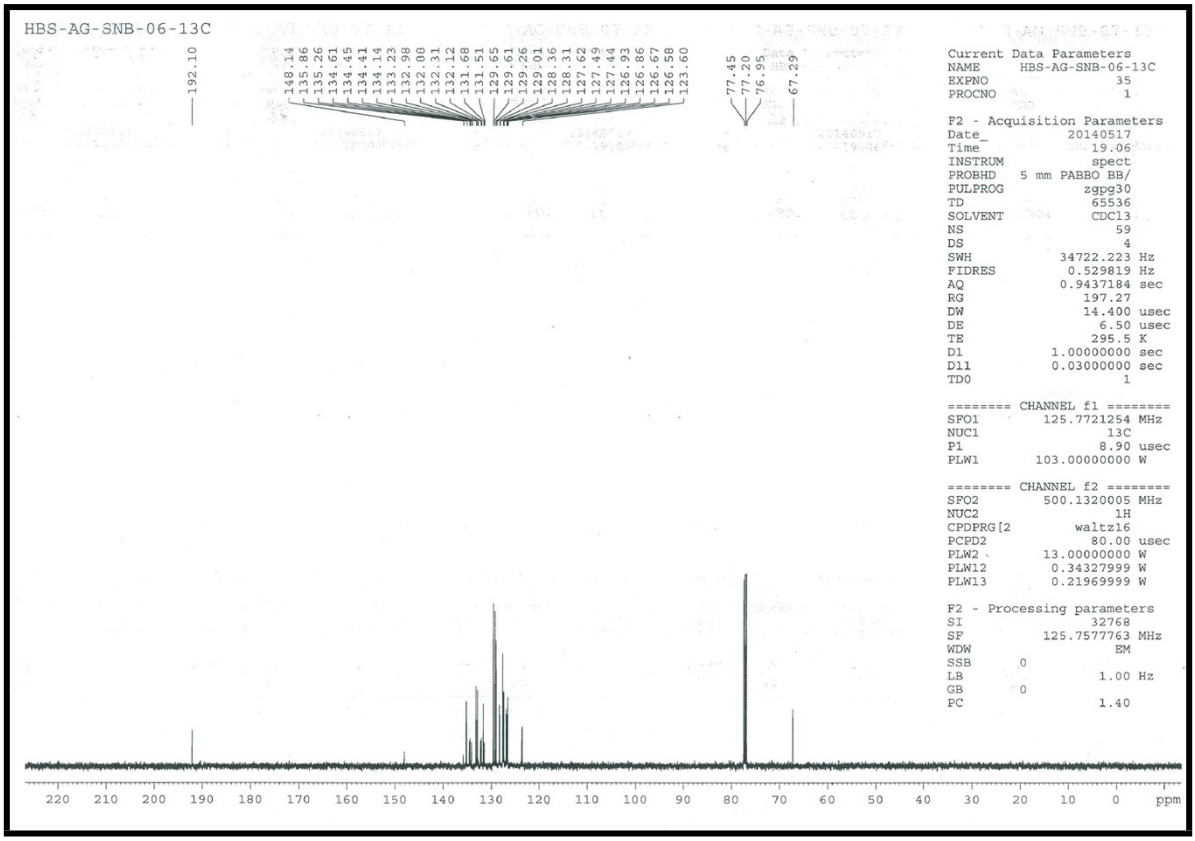

Fig. S27 ^{13}C NMR spectrum of [(*1*-$C_{10}H_7$)-{$C_6H_5C(Br)=CH$}]$TeBr_2$ (**6**).

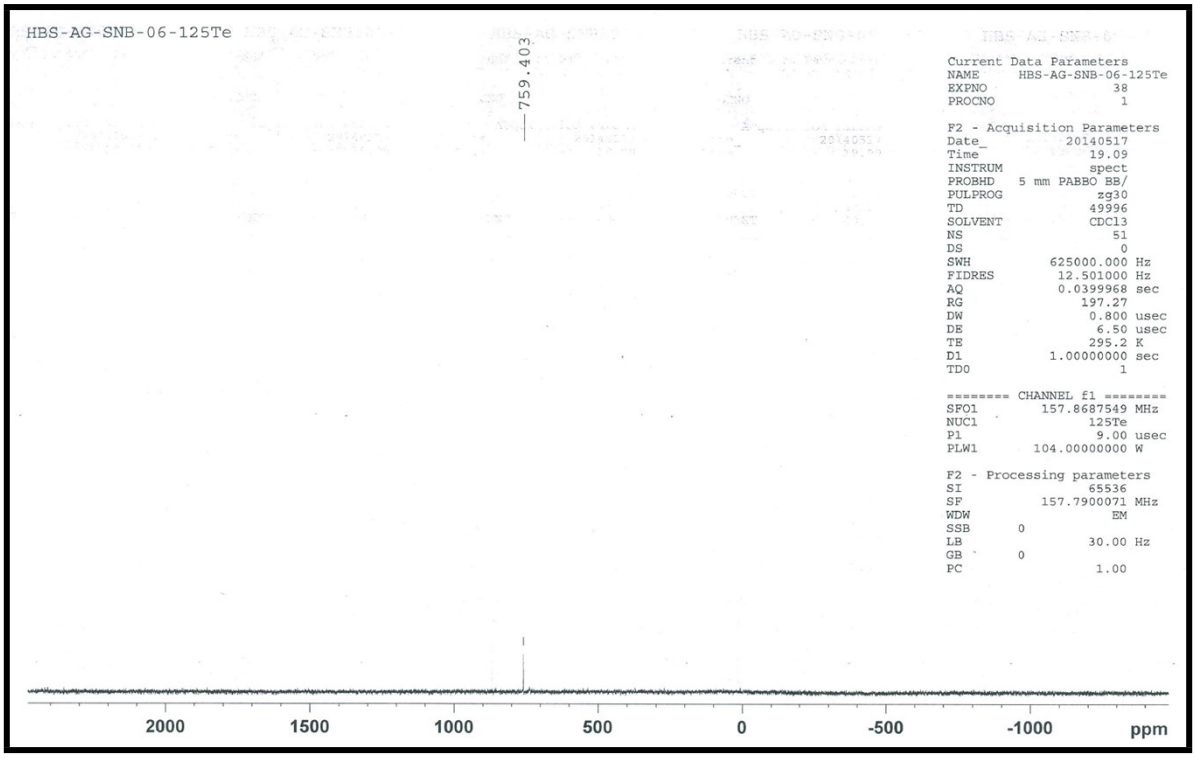

Fig. S28 ^{125}Te NMR spectrum of [(*1*-$C_{10}H_7$)-{$C_6H_5C(Br)=CH$}]$TeBr_2$ (**6**).

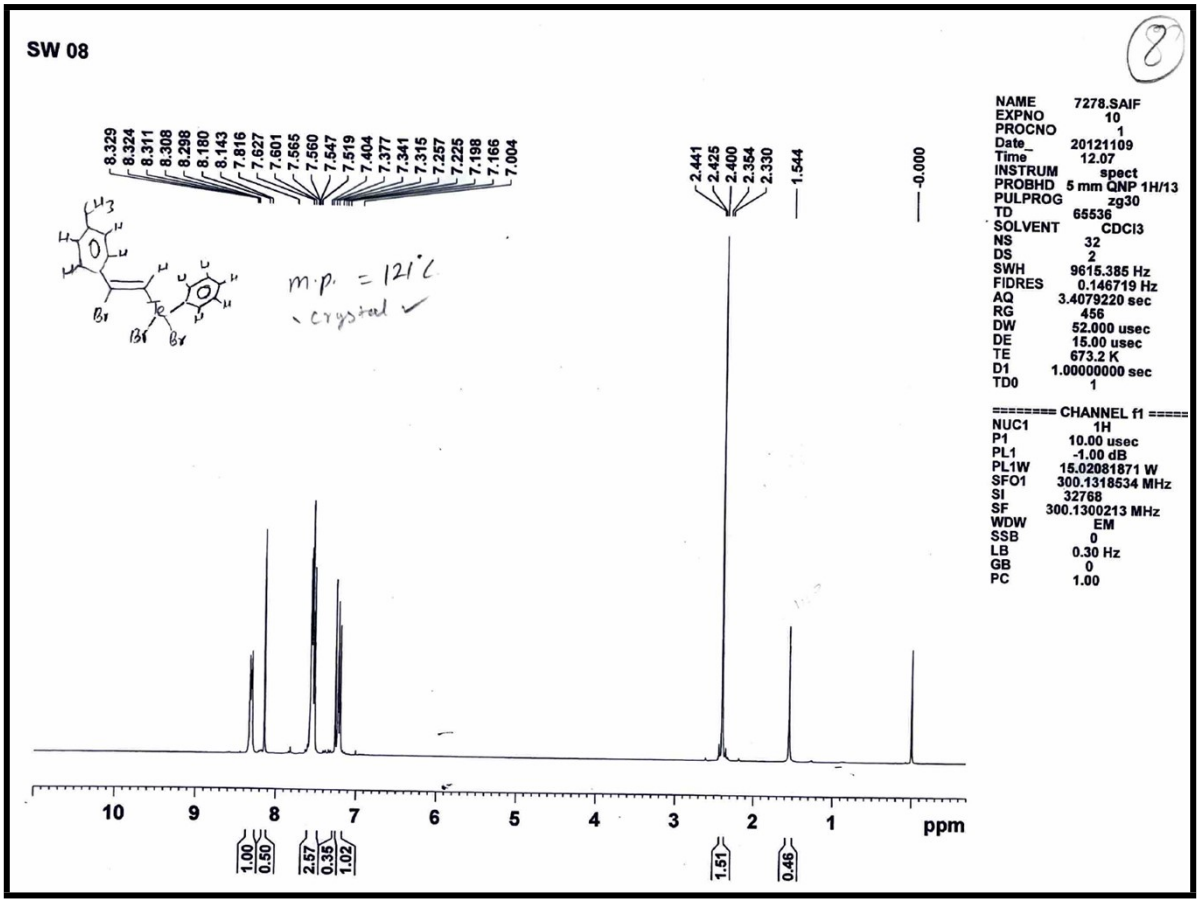

Fig. S29 ^{1}H NMR spectrum of [(C_6H_5)-{*4*-CH_3-C_6H_4C(Br)=CH}]$TeBr_2$ (**7**).

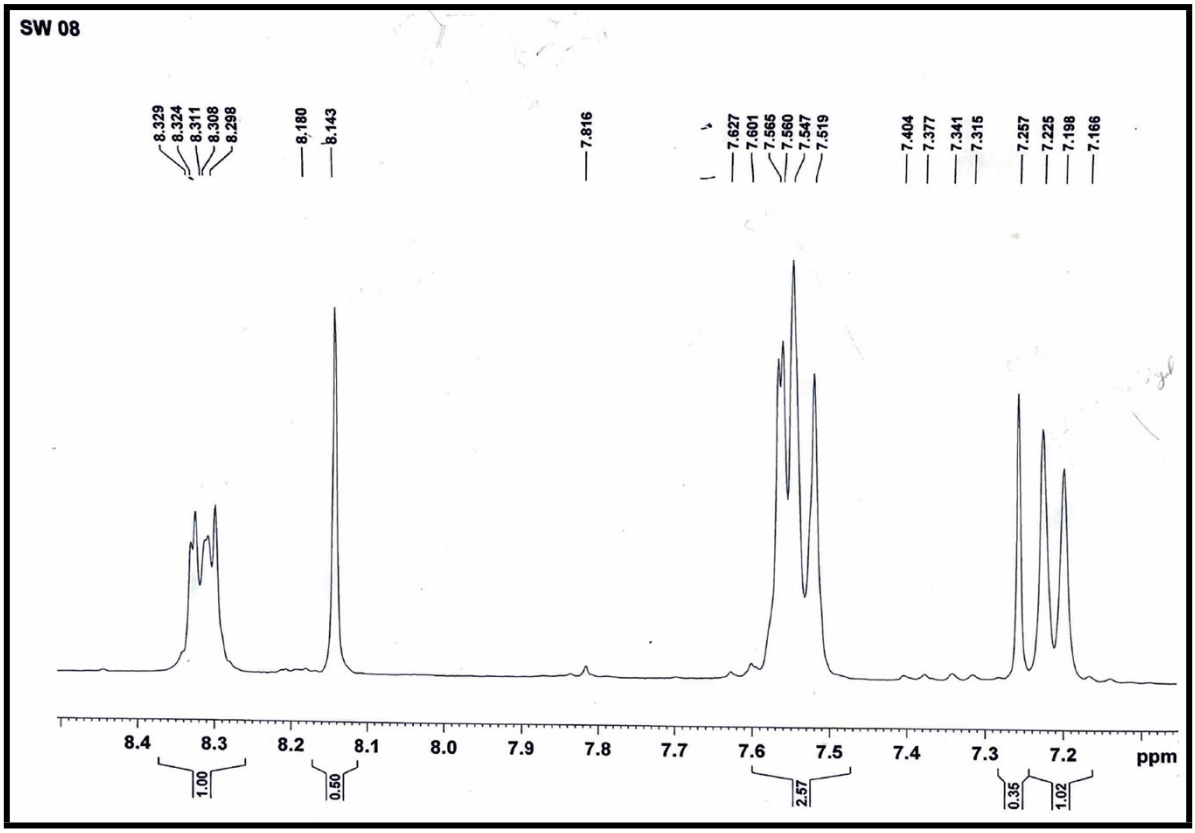

Fig. S30 Expanded aryl region ^{1}H NMR spectrum of [(C_6H_5)-{*4*-CH_3-C_6H_4C(Br)=CH}]$TeBr_2$ (**7**).

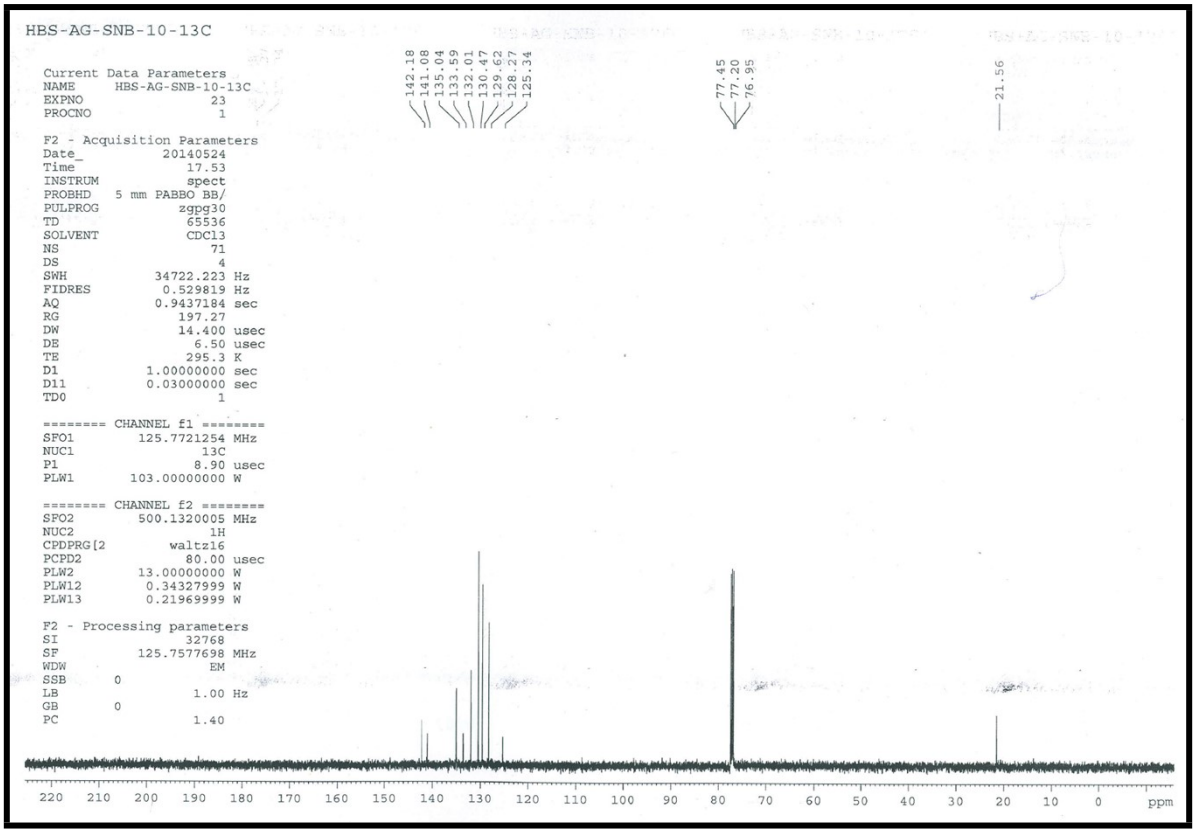

Fig. S31 ^{13}C NMR spectrum of [(C_6H_5)-{*4*-CH_3-C_6H_4C(Br)=CH}]$TeBr_2$ (**7**).

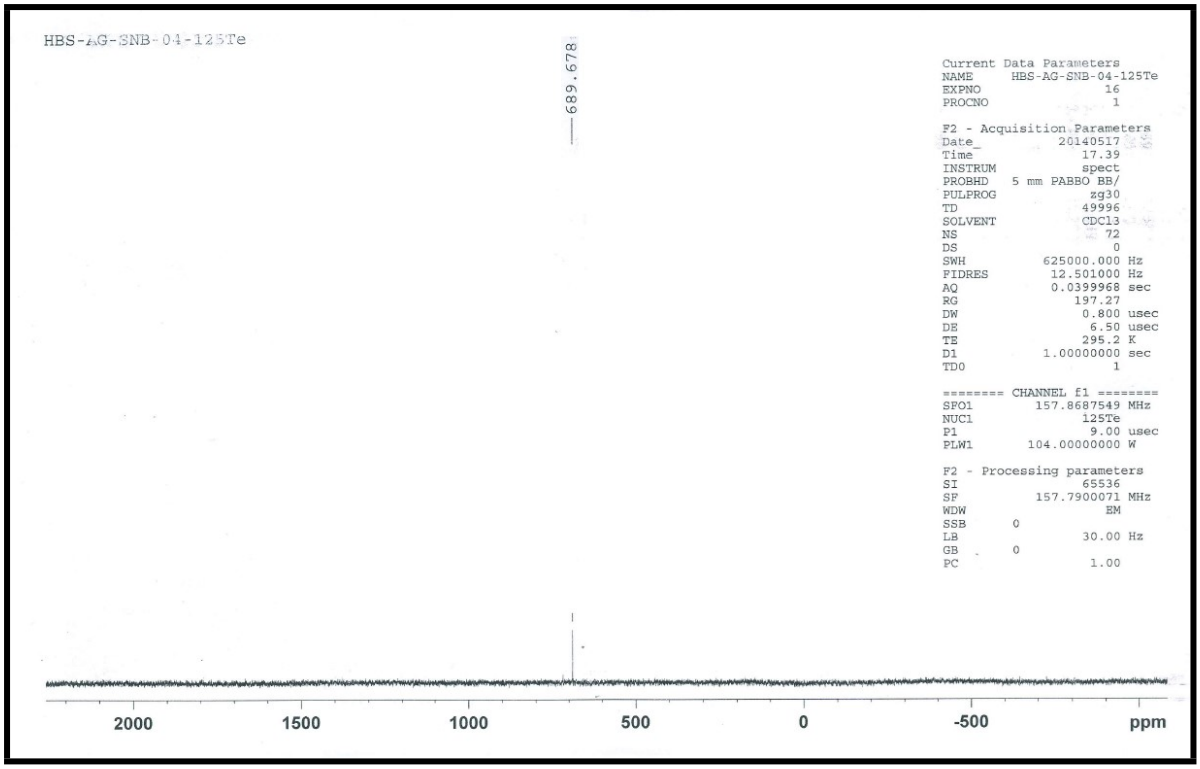

Fig. S32 ^{1253}Te NMR spectrum of [(C_6H_5)-{*4*-CH_3-C_6H_4C(Br)=CH}]$TeBr_2$ (**7**).

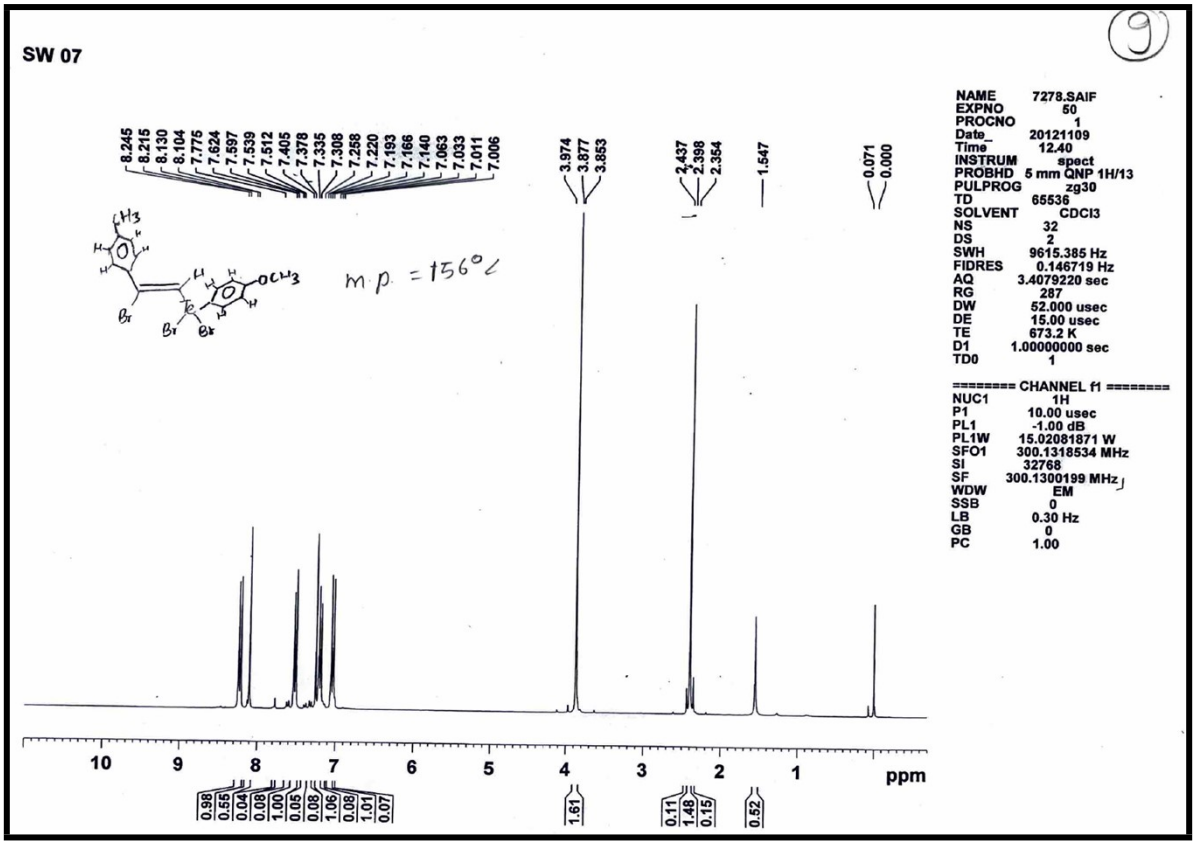

Fig. S33 ^{1}H NMR spectrum of [(*4*-CH_3O-C_6H_4)-{*4*-CH_3-$C_6H_4C(Br)=CH$}]$TeBr_2$ (**8**).

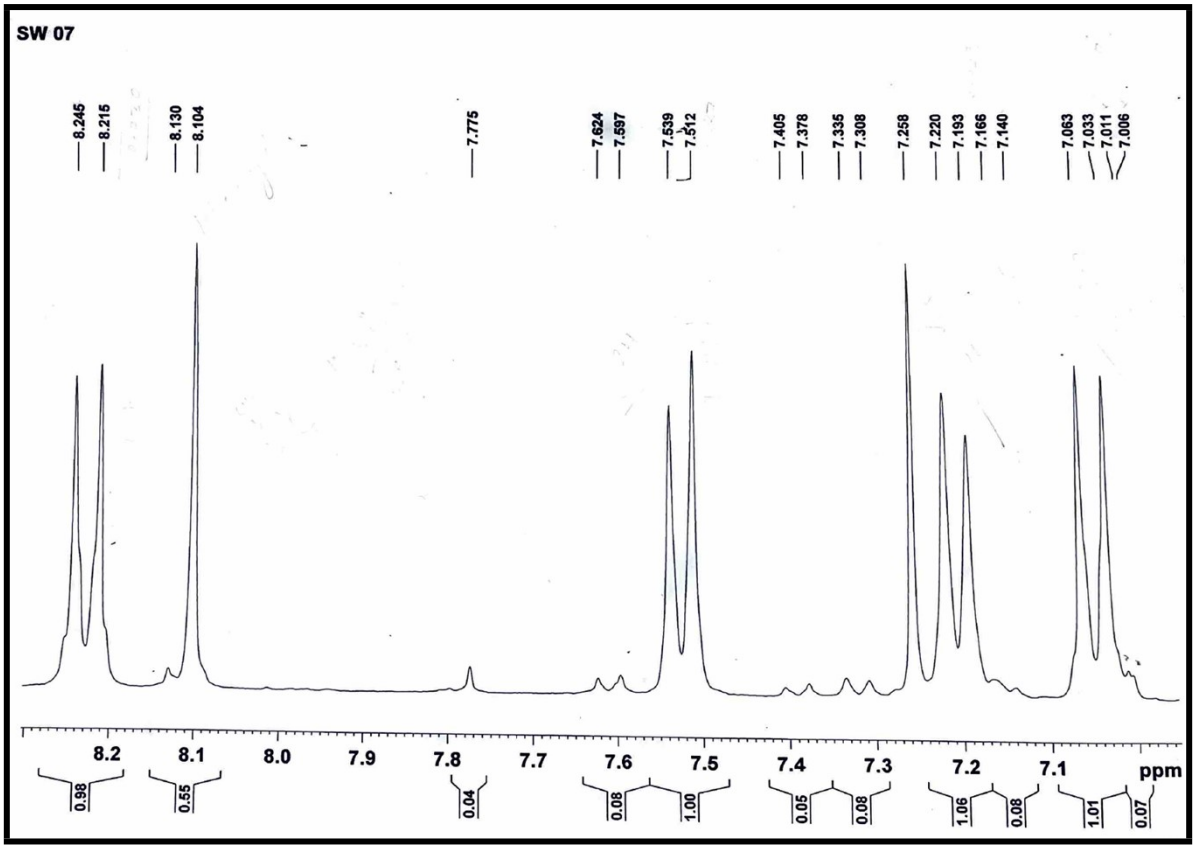

Fig. S34 Expanded aryl region ^{1}H NMR spectrum of [(*4*-CH_3O-C_6H_4)-{*4*-CH_3-$C_6H_4C(Br)=CH$}]$TeBr_2$ (**8**).

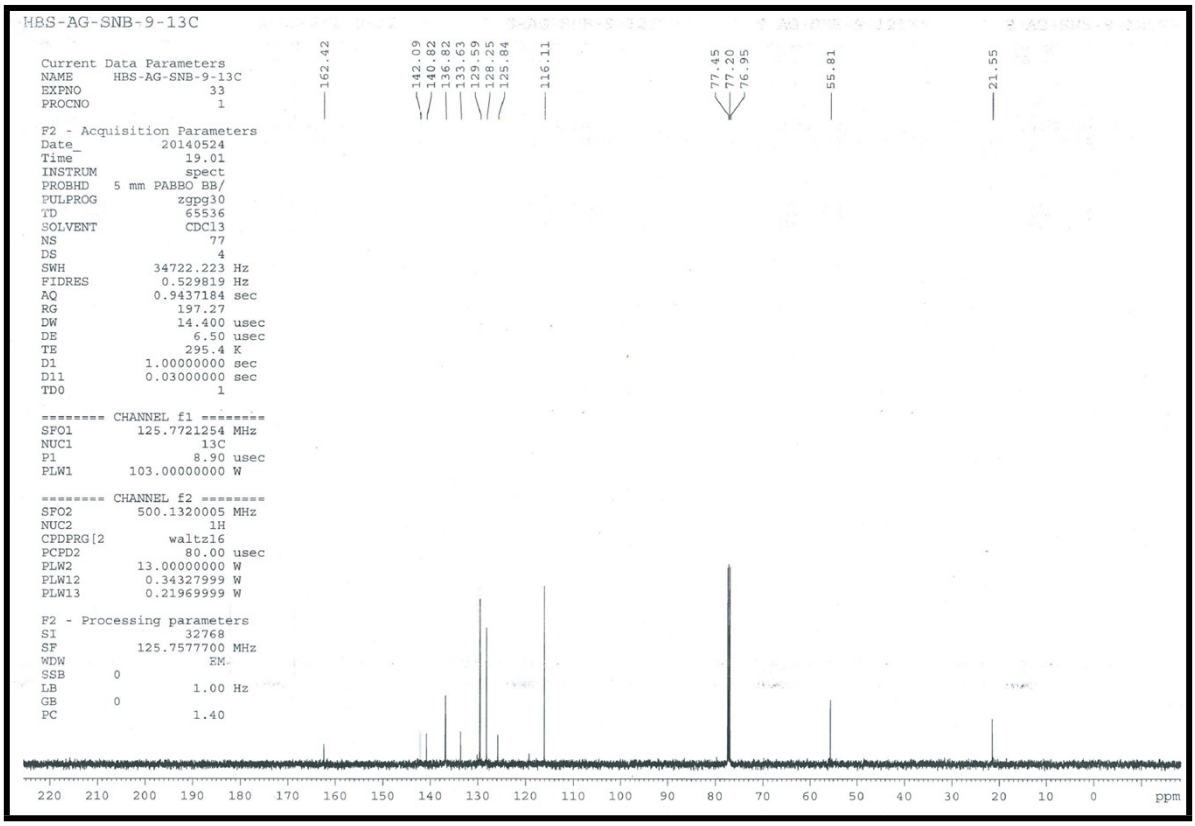

Fig. S35 ^{13}C NMR spectrum of [(*4*-CH_3O-C_6H_4)-{*4*-CH_3-$C_6H_4C(Br)=CH$}]$TeBr_2$ (**8**).

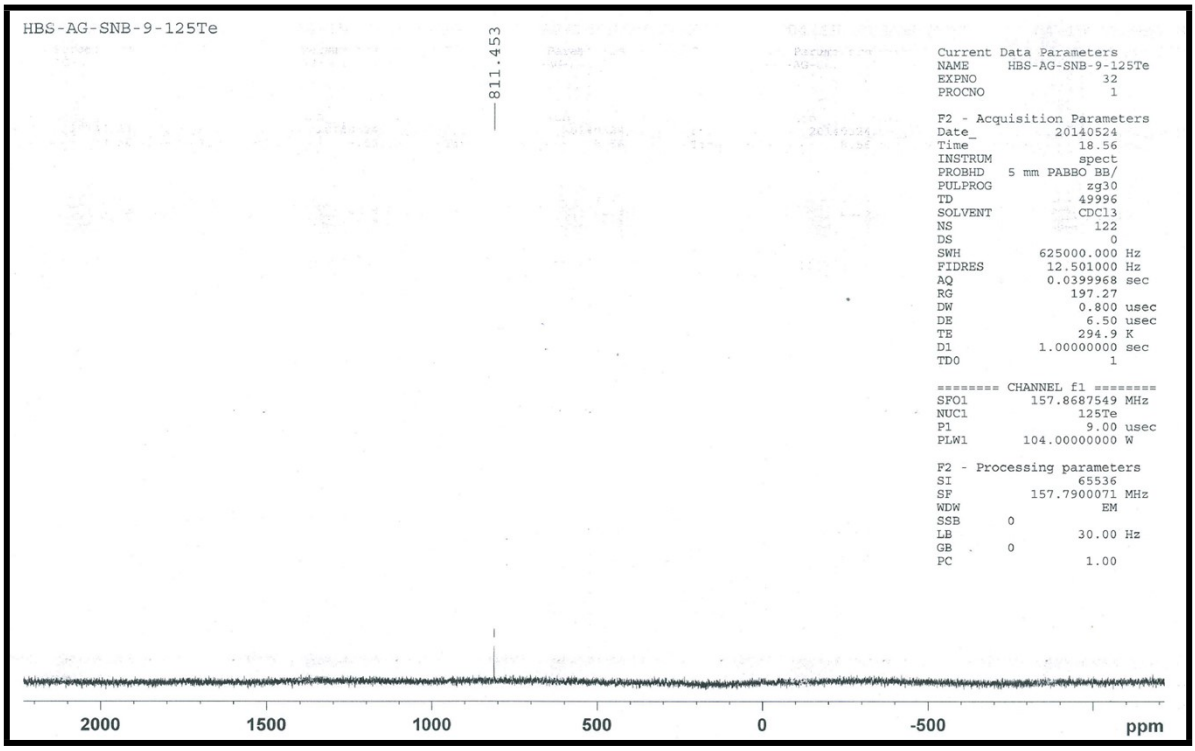

Fig. S36 ^{125}Te NMR spectrum of [(*4*-CH_3O-C_6H_4)-{*4*-CH_3-$C_6H_4C(Br)=CH$}]$TeBr_2$ (**8**).

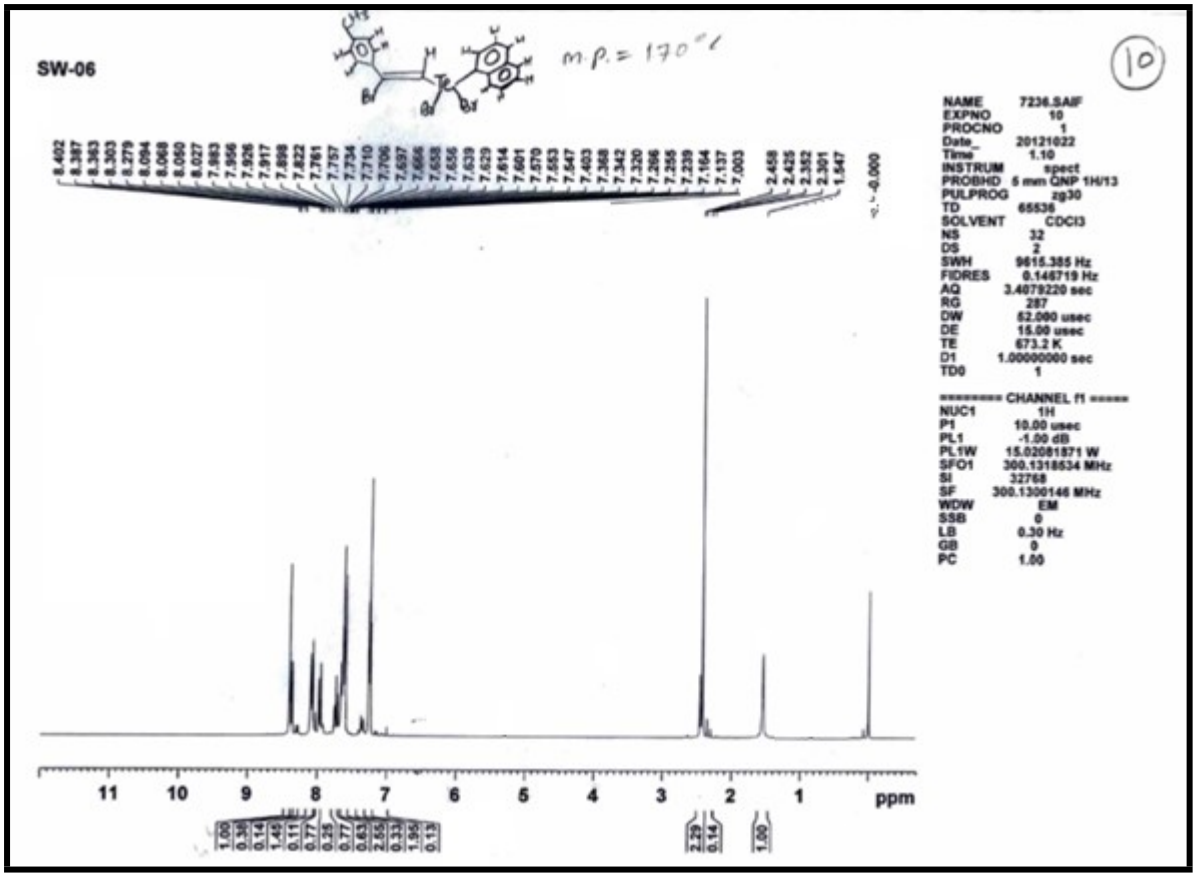

Fig. S37 ^{1}H NMR spectrum of [(*1*-$C_{10}H_7$)-{*4*-CH_3-$C_6H_4C(Br)=CH$}]$TeBr_2$ (**9**).

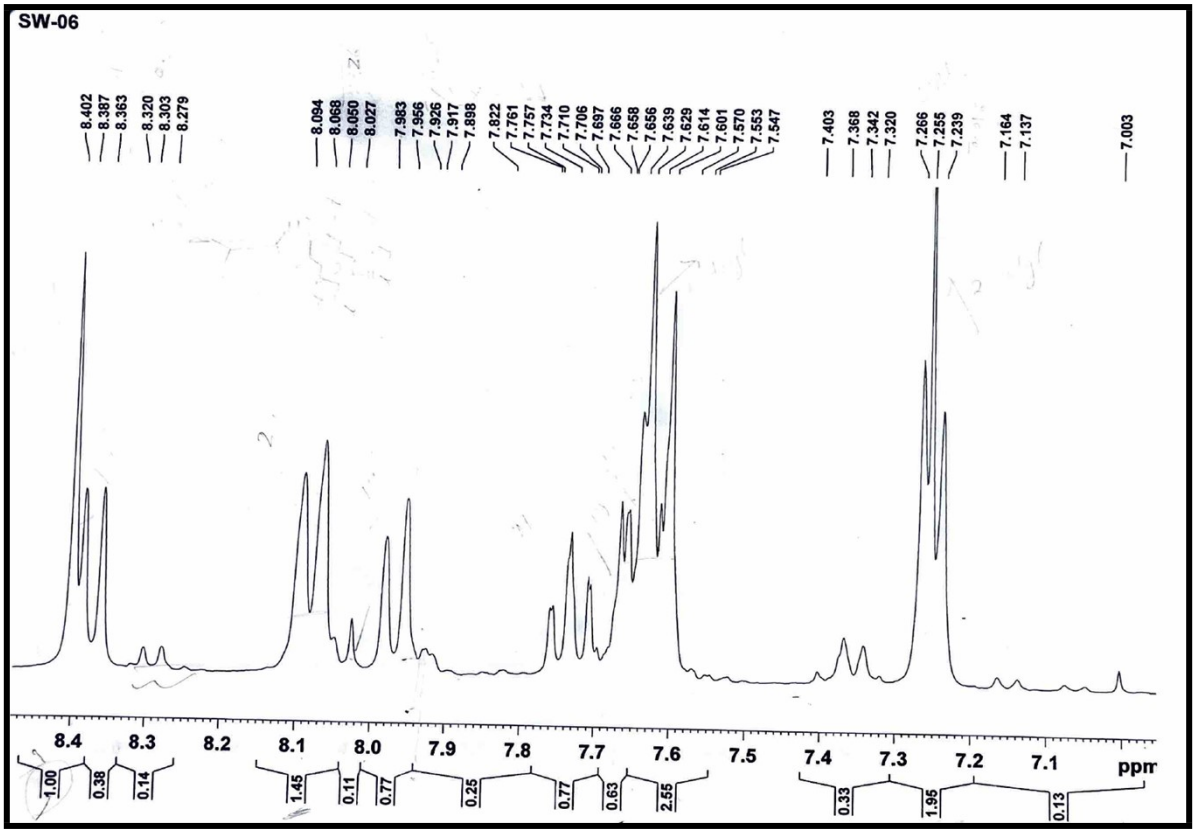

Fig. S38 Expanded aryl region ^{1}H NMR spectrum of [(*1*-$C_{10}H_7$)-{*4*-CH_3-$C_6H_4C(Br)=CH$}]$TeBr_2$ (**9**).

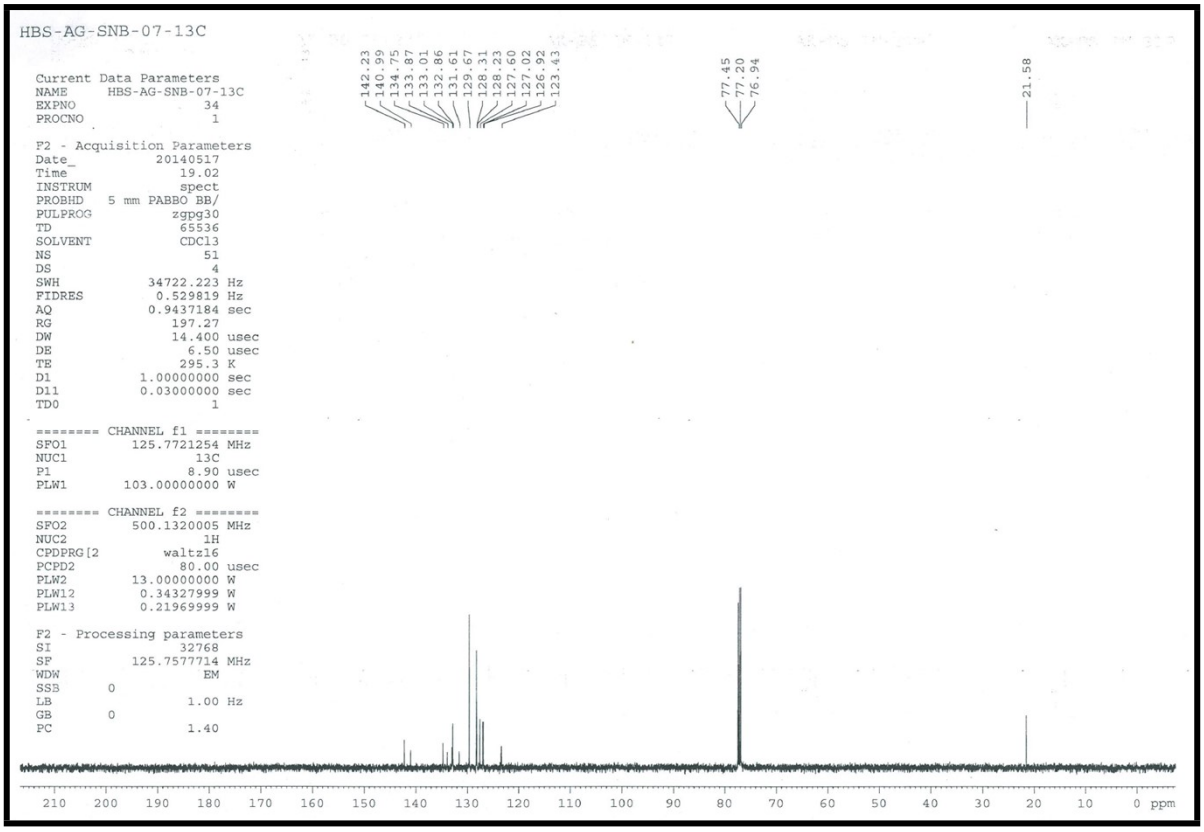

Fig. S39 ^{13}C NMR spectrum of [(*1*-$C_{10}H_7$)-{*4*-CH_3-C_6H_4C(Br)=CH}]$TeBr_2$ (**9**).

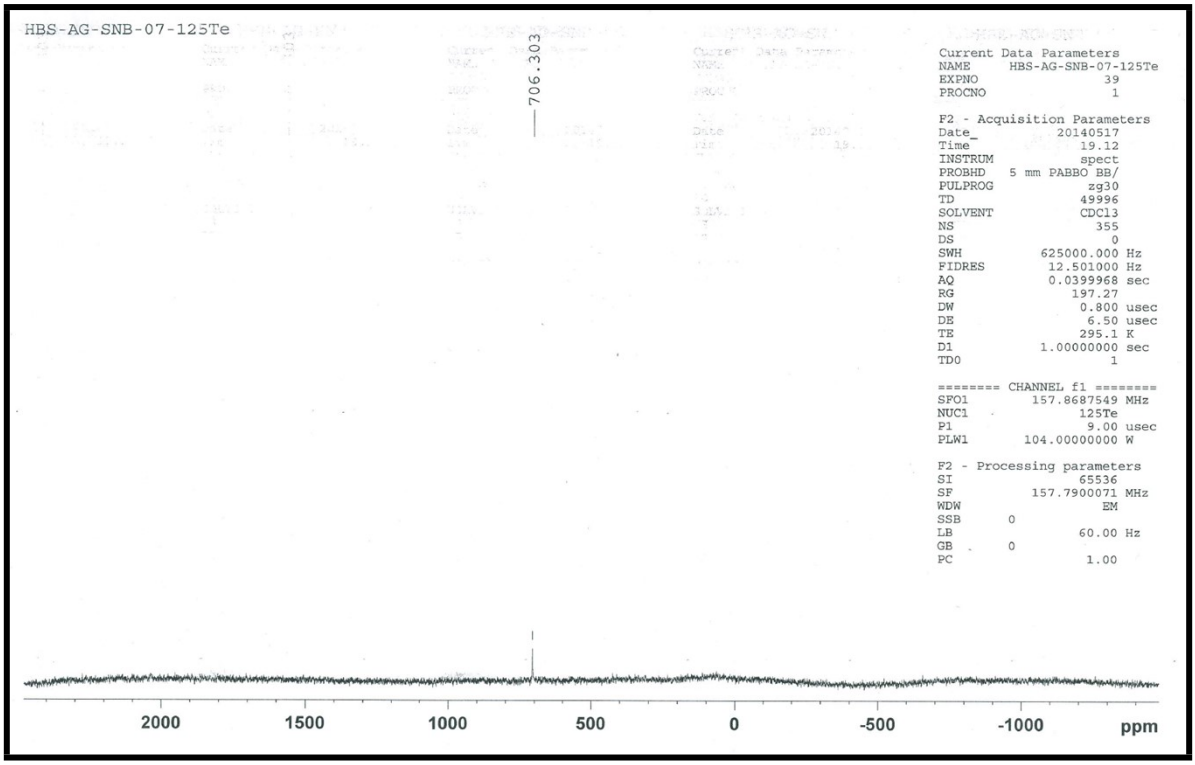

Fig. S40 ^{125}Te NMR spectrum of [(*1*-$C_{10}H_7$)-{*4*-CH_3-C_6H_4C(Br)=CH}]$TeBr_2$ (**9**).